Disorder driven roughening transitions of elastic manifolds and periodic elastic media[*]

T. Emig[a] and T. Nattermann

Institut für Theoretische Physik, Universität zu Köln, Zülpicher Strasse 77, 50937 Köln, Germany

Abstract. The simultaneous effect of both disorder and crystal-lattice pinning on the equilibrium behavior of oriented elastic objects is studied using scaling arguments and a functional renormalization group technique. Our analysis applies to elastic manifolds, *e.g.*, interfaces, as well as to periodic elastic media, *e.g.*, charge-density waves or flux-line lattices. The competition between both pinning mechanisms leads to a continuous, disorder driven roughening transition between a flat state where the mean relative displacement saturates on large scales and a rough state with diverging relative displacement. The transition can be approached by changing the impurity concentration or, indirectly, by tuning the temperature since the pinning strengths of the random and crystal potential have in general a different temperature dependence. For D dimensional elastic manifolds interacting with either random-field or random-bond disorder a transition exists for $2 < D < 4$, and the critical exponents are obtained to lowest order in $\epsilon = 4 - D$. At the transition, the manifolds show a superuniversal logarithmic roughness. Dipolar interactions render lattice effects relevant also in the physical case of $D = 2$. For periodic elastic media, a roughening transition exists only if the ratio p of the periodicities of the medium and the crystal lattice exceeds the critical value $p_c = 6/\pi\sqrt{\epsilon}$. For $p < p_c$ the medium is always flat. Critical exponents are calculated in a double expansion in $\mu = p^2/p_c^2 - 1$ and $\epsilon = 4 - D$ and fulfill the scaling relations of random field models.

PACS. 68.35.Ct Interface structure and roughness – 71.45.Lr Charge-density-wave systems – 64.70.Rh Commensurate-incommensurate transitions – 68.35.Rh Phase transitions and critical phenomena – 05.20.-y Statistical mechanics – 74.60.Ge Flux pinning, flux creep, and flux-line lattice dynamics

1 Introduction

The thermal roughening transition (RT) from a faceted to a smooth surface of a crystal is one of the paradigms of condensed matter physics [1]. It has been observed directly for a number of materials, in particular on surfaces of crystalline Helium 4 [2]. A similar transition occurs between a rough delocalized and a flat localized state of the interface in the three-dimensional Ising and related lattice models [3,4]. At the RT temperature T_R the free energy of a step on the surface vanishes. Apart from its shape also other physical properties are influenced by the presence of the RT, *e.g.*, the growth (drift) velocity u of the crystal surface (interface) changes dramatically at the RT from $u \sim \exp(-C/f)$ for $T < T_R$ to $u \sim f$ for $T > T_R$ [2]. Here f denotes the driving force density, which is proportional to the difference $\Delta\mu$ of the chemical potentials of the crystal and its melt in the case of crystal growth and the magnetic field in the case of Ising magnets, respectively.

A third closely related example for the RTs are the lock-in transitions of periodically modulated structures into an underlying crystalline matrix. Examples for the modulated structures are spin or charge density waves (CDWs) in anisotropic metals [5,6], mass density waves in superionic conductors [7], polarization density waves in incommensurate ferrolectrics [8], Wigner crystals [9], magnetic bubble arrays [10], flux line lattices (FLLs) [11, 12] and nematic elastomers [13], *etc.* The phenomenology of these bulk systems is even more rich than that of sur- or interfaces, since in general a large number of different locked-in structures separated by incommensurate phases may occur.

Common feature of the examples mentioned is the existence of a D-dimensional deform-able object (*i.e.* $D = 1$ for single flux lines, $D = 2$ for surfaces or interfaces, $D = 3$ for CDWs or the FLL *etc.*) the energy of which – in the absence of lattice effects – can be described by elasticity theory. The distortion of the elastic object is expressed in general by an N-component displacement field $\phi^i(\mathbf{x}), i = 1, ..., N$, where $N = 1$ for surfaces, interfaces and CDWs, $N = 2$ for flux lines or FLLs *etc.* These elastic objects interact with the potential of the underlying crystalline matrix, which favors (in a commensurate situation)

---

[a] e-mail: `te@thp.uni-koeln.de`

certain spatially homogeneous ("flat") configurations because of their lower energy E. On the other hand, thermal fluctuations favor a spatially inhomogeneous ("rough") configuration because these have the higher entropy S. The real macroscopic configuration is that of the lowest free energy $F = E - TS$, from which we expect the occurrence of a roughening transition at a temperature $T = T_R$.

Later we will subdivide these elastic objects into *manifolds*, which comprise single flux lines or domain walls, and *periodic media*, *i.e.* periodic lattices of flux lines or domain walls, CDWs *etc.* This distinction will become necessary because manifolds and periodic media couple in different ways to the disorder. However, a distinction is unnecessary as long as we consider merely thermal fluctuations.

The interest in the investigation of the roughening transition goes also beyond its immediate applications in condensed matter physics. In computer simulations of condensed matter systems a *fake* periodic lattice potential – in addition to that of the crystalline matrix – appears frequently in the form of a grid on which the simulations are done, which has nothing to do with the physics of the problem. In order to retrieve physically relevant informations from these simulations one has to make sure to be above the roughening transition of this fake potential. This remark applies also to lattice gauge theories in high energy physics [14,15].

Besides of its frequent occurrence the second interesting aspect of the thermal RT is its *universality*. Although the RT temperature T_R itself is non-universal and depends in particular on the elastic properties of the object under consideration (*e.g.* on the orientation of a vicinal surface relative to the main crystalline axes), the universal features like the singular behavior of the thermodynamic quantities are the same for all models with the same spatial dimension D and number of field components N. Moreover, the thermal RT for $D = 2$-dimensional surfaces was shown to be in the same universality class as the metal-insulator transition of a 2D-Coulomb gas [16], the Kosterlitz-Thouless transition of a 2D XY-model [17] (both with an inverted temperature axis), the phase transition of the 2D sine-Gordon model [18] and the transition of the 1D XXZ-chain at $T = 0$ [19].

$D = 2$ is indeed the upper critical dimension for the thermal RT since $D > 2$ dimensional manifolds are flat even without a lattice potential.

Interesting but less known is the fact that Kosterlitz [20] and Forgacs *et al.* [21] considered the thermal RT for $1 < D \leq 2$ interface dimensions and found a superuniversal (*i.e.* dimension independent) logarithmic roughness *at* the transition. Finally, the thermal RT disappears in $D = 1$ dimensions: 1-dimensional interfaces are rough at all finite T [22].

Disorder is an even more efficient source of roughening of manifolds than thermal fluctuations and physically important as well [23].

Roughening of interfaces due to disorder was considered to determine the lower critical dimension of the random field Ising model [24–26] and the mobility of domain walls in disordered magnets [27–32]. It was argued that in the presence of disorder interfaces of dimensions $D \leq 2$ are always rough, but undergo a roughening transition as a function of the disorder strength for $D > 2$ dimensions [33,34]. Bouchaud and Georges [35] considered explicitly the competition between lattice and impurity pinning in $2 \leq D \leq 4$ dimensions using a variational calculation. Surprisingly they found *three* phases: a weakly disordered flat, a rough glassy and an intermediate flat phase with strong glassy behavior. For $D \leq 2$ only the glassy rough phase was expected to survive, but that cross-over regions of the two other phases would still be seen in the short scale behavior. However, it should be kept in mind that the variational calculation is an uncontrolled approximation and typically reproduces the results obtained from Flory-like arguments.

It is the aim of the present paper to give a unified renormalization group description of the roughening transition of elastic manifolds and periodic media in the presence of quenched disorder. Some preliminary results were already published [36,37]. In this paper we focus on the derivation of the renormalization group flow equations and their solutions for the different cases. To make the paper more self-contained some of the results reported already in references [36,37] are included here as well. The physics is complicated by the occurrence of various input length scales like the periodicity of the crystalline matrix a_0/p, the correlation length of the disorder ξ_0 and the periodicity of the periodic medium l.

The outline of the paper is as follows. In Section 2 the model for the pinned elastic objects is described. The different classes of disorder correlations are briefly reviewed. Section 3 analyses the model on the basis of simple scaling arguments. A qualitative picture of the phase diagram is developed and the characteristic length scales are identified. In Section 4 we proceed with the derivation of the functional RG equations to lowest order in $D = 4 - \epsilon$ dimensions. The functional RG flow of the disorder correlator is reduced to a flow of single parameters in Section 5. The fixed points of this RG flow are analyzed for vanishing lattice potential, reproducing the known results. The effect of a finite lattice potential is considered in Section 6. The critical exponents of the resulting roughening transition are calculated to lowest order in ϵ for the different types of disorder. Experimental implications of our results and related recent experiments are discussed in Section 7. The last section concludes with a summary and discussion of our results and briefly comments on related open questions not treated in this paper.

2 The model

As mentioned already in the Introduction, the elastic objects are described by an N-component phase field $\boldsymbol{\phi}(\mathbf{x})$ with components $\phi^i(\mathbf{x})$, $i = 1, \ldots, N$, which interacts both with an underlying periodic crystalline lattice potential $V_L(\boldsymbol{\phi})$ and a random potential $V_R(\boldsymbol{\phi}, \mathbf{x})$ specified

Table 1. Different physical realizations of the model (1); topological defects are excluded.

Elastic object	d	D	N	ϕ	p	$R_0(\phi)$, $|\phi| \gg \xi_0$
Interface [24–26]	≥ 2	$d-1$	1	$2\pi u/a$ u displacement	1	$-|\phi|$ (random field) $e^{-\phi^2/\xi_0^2}$ (random bond)
density wave [6–8]	≥ 2	d	1	$\delta\rho(\mathbf{x}) = \rho_1 \cos(\mathbf{qx}+\phi)$	$\mathbf{q} = \mathbf{Q}/p$	$\cos\phi$
XY–magnet in crystal and random field	≥ 2	d	1	$\arctan(S_y/S_x)$	≥ 1, number of easy directions	$\cos\phi$
flux line lattice [11,12]	≥ 2	d	2	$2\pi\mathbf{u}/l$ l flux line spacing	$p = l/a$	$\sum_{\mathbf{Q}\neq\mathbf{0}} R_{\mathbf{Q}}\cos(\mathbf{Q}\phi)$ $\mathbf{Q}$ reciprocal lattice vectors
^{4}He surface in aerogel	≥ 2	$d-1$	1	$2\pi h/a$ h height variable	1	$-|\phi|$
nematic elastomer in external and random field [13]	≥ 2	d	1	$\arctan(n_y/n_x)$ $\mathbf{n}$ unit director field	1	$\cos\phi$

below. The total Hamiltonian is then given by

$$\mathcal{H} = \gamma \int d^D\mathbf{x} \left\{ \frac{1}{2}\boldsymbol{\nabla}\phi \cdot \boldsymbol{\nabla}\phi - V_L(\phi(\mathbf{x})) - V_R(\phi(\mathbf{x}),\mathbf{x}) \right\}. \tag{1}$$

The strength of the pinning potentials is measured in units of the elastic stiffness constant γ which controls isotropic elastic deformations. More complicated elastic moduli could be considered but turn out to be unessential as long as we are interested in universal properties. For manifold models, the elastic object is embedded into a larger space of dimension $d = D + N$ whereas for periodic media the dimension of the space in which the elastic structure is embedded is equal to the internal dimension, $d = D$. The different realizations of the model (1) are summarized in Table 1.

The periodic potential $V_L(\phi)$ can be rewritten as

$$V_L(\phi) = \sum_{i=1}^{N} V(\phi^i). \tag{2}$$

if the original crystalline matrix is assumed to have the symmetry of an N–dimensional hyper–cubic lattice with spacing a_0. Below we will measure all length scales in units of a_0, *i.e.* we will put $a_0 \equiv 1$. The resulting $V(\phi^i)$ is then a periodic function of periodicity $2\pi/p$. The random pinning potential $V_R(\phi,\mathbf{x})$ is assumed to be Gaussian distributed with a vanishing average $\overline{V_R(\phi,\mathbf{x})} = 0$ and two-point correlation function

$$\overline{V_R(\phi,\mathbf{x})V_R(\phi',\mathbf{x}')} = R(\phi-\phi')\delta^{(D)}(\mathbf{x}-\mathbf{x}'). \tag{3}$$

The starting point for our further calculations is the replica Hamiltonian $\mathcal{H}_n$, which follows, *e.g.*, from the con-

sideration of the disorder averaged free energy

$$\overline{F} = -T \lim_{n\to 0} \frac{1}{n} \left(\text{Tr} e^{-\mathcal{H}_n} - 1 \right) \tag{4}$$

with

$$\mathcal{H}_n = \frac{\gamma}{T} \sum_{\alpha\beta=1}^{n} \int d^D x \left\{ \left[\frac{1}{2}\boldsymbol{\nabla}\phi_\alpha \cdot \boldsymbol{\nabla}\phi_\beta - V_L(\phi_\alpha) \right] \delta_{\alpha\beta} - \frac{\gamma}{2T} R(\phi_\alpha - \phi_\beta) \right\}. \tag{5}$$

The actual form of the disorder correlator $R(\phi)$ depends on the type of disorder and on the model under consideration.

We give here a brief discussion of the main classes of disorder correlators:

For *elastic manifolds* one has to distinguish between random field and random bond systems.

(i) For *random field system* [24,25] the bare disorder correlator is given by

$$R_0(\phi) = -\Delta_0 \begin{cases} |\phi|\xi_0 & \text{for } |\phi| \gg \xi_0 \\ \phi^2 & \text{for } |\phi| \ll \xi_0 \end{cases}. \tag{6}$$

Here $\sqrt{\Delta_0}$ denotes the strength of the random field, Δ_0 is proportional to the concentration n_{imp} of the random field impurities. ξ_0 is of the order of the maximum of the intrinsic domain wall width and the correlation length of the random field. The result (6) was derived in [24,25] for $N = 1$ component fields. Its formal generalization to arbitrary $N > 1$ is straightforward but without direct physical application. However, this case will be included here in order to enable the comparison of our results with that of

the variational approach of Bouchaud and Georges [35] which is expected to become exact for $N \to \infty$.

As an other interesting realization of a sine-Gordon model with random field disorder, we suggest surfaces of crystalline ^{4}He in an aerogel. Here the silica strands act as quenched impurities on the crystal surface. Fractal correlations in the aerogel density appearing on short scales should be negligible if the correlation length $\xi_\parallel$ of the surface exceeds all structural length scales of the aerogel.

(ii) For *random bond systems* with short range correlations in the disorder the bare disorder correlator is given by

$$R_0(\phi) = \Delta_0 \xi_0^2 \exp(-\phi^2/2\xi_0^2). \qquad (7)$$

The length ξ_0 has the same meaning here as for random field systems. Note that in our notation ξ_0^2 includes a factor N such that ξ_0^2/N remains finite in the limit $N \to \infty$.

(iii) In the case of *periodic elastic media* the form of the bare disorder correlator is dominated by the periodicity of the elastic medium. To show this more explicitly we start, for simplicity, with a scalar field ϕ. The periodically modulated density can be expanded in a Fourier series

$$\rho(\mathbf{x}, \phi) = \sum_{m=0}^{\infty} \rho_m \cos[m(\mathbf{qx} + \phi(\mathbf{x}))] \qquad (8)$$

where $\mathbf{q}$ denotes the modulation vector of the locked–in phase. The coupling to the disorder potential $U(\mathbf{x})$ is of the form

$$V_R(\phi, \mathbf{x}) = U(\mathbf{x})\rho(\mathbf{x}, \phi) \qquad (9)$$

where $U(\mathbf{x}) = U_0 \left(\sum_i \delta(\mathbf{x} - \mathbf{x}_i) - n_{imp}\right)$. Here $\mathbf{x}_i$ and n_{imp} are the positions and the concentration of the impurities. The disorder average is performed by integration over all possible impurity positions,

$$\overline{A} \equiv \prod_i \int \frac{d^D x_i}{\mathcal{V}} A(\{x_i\}). \qquad (10)$$

Here the integration extends over the volume $\mathcal{V}$ of the system. With (3, 8, 9) and neglecting rapidly oscillating terms we get then in a straightforward manner

$$R_0(\phi) = \frac{1}{2} n_{\mathrm{imp}} U_0^2 \sum_{m=0}^{\infty} \rho_m^2 \cos(m\phi). \qquad (11)$$

This expression can be extended to vector fields $\phi(\mathbf{x})$ as discussed by Giamarchi and Le Doussal [38] in the context of flux line arrays in superconductors, and gives

$$R_0(\phi) = \sum_{\mathbf{Q} \neq \mathbf{0}} R_{\mathbf{Q}} \cos(\mathbf{Q}\phi) \qquad (12)$$

with Fourier coefficients $R_{\mathbf{Q}}$ [39] where $\mathbf{Q}$ are the reciprocal lattice vectors of the periodic medium. Generally, rewriting the periodic density $\rho(\mathbf{x}, \phi)$ in terms of a displacement field ϕ, also gradient terms of the form $-\rho_0 \sum_{i=1}^{N} \partial_i \phi^i$ are generated in equation (8) which lead to terms of the form $\partial_i \phi_\alpha^i \partial_j \phi_\beta^j$ in equation (5). But these gradient terms can be shown to be strongly irrelevant for the large distance behavior for $D > 2$ [39]. Therefore, in the following this interaction will be neglected.
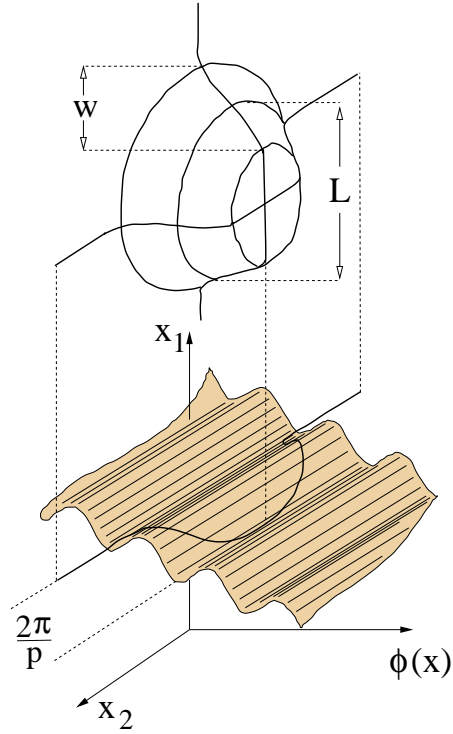
Fig. 1. Two-dimensional manifold forming a terrace to gain energy from the random potential without any bulk energy cost from the periodic potential.

3 Scaling arguments

In this section we present some elementary scaling considerations for the system described by the Hamiltonian (1), which give a qualitative picture of the phase diagram, the critical dimensions and the characteristic length scales. Since we are interested only in qualitative estimates, we neglect all numerical factors of order unity.

We start with the *elastic manifolds* and restrict our analysis to the interface case $N = 1$. The extension to $N > 1$ does not change the qualitative conclusions derived for $N = 1$. Since disorder fluctuations turn out to be much stronger than those of thermal fluctuations, we put $T = 0$ from the very beginning, postponing the discussion of the influence of finite temperatures to the end of this section.

In the absence of disorder, $\Delta_0 = 0$, the interface is flat. Typical excitations consist of terraces of height $2\pi/p$ and linear extension L. The terraces are bound by steps of width $w \approx 1/p\sqrt{v_0}$ and energy $E_{step} \simeq \gamma\sqrt{v_0}L^{D-1}/p$ where we used for simplicity $V_L(\phi) \simeq v_0 \cos p\phi$ for the lattice potential, see Figure 1. Disorder can lower the energy of terraces since the locally displaced interface sees a different random potential. To be specific, we find for the energy of a hump of total height ϕ consisting of $\phi p/2\pi$ steps

$$E_{total}/\gamma \simeq \sqrt{v_0}L^{D-1}\phi - \sqrt{\Delta_0 \xi_0 L^D \phi}. \qquad (13)$$

The second part represents the energy gain from the random field. Minimizing the total energy (13) with respect

to ϕ we obtain $p\phi \simeq (L/L_R)^{2-D}$ with

$$L_R \simeq (v_0/\xi_0\Delta_0 p)^{1/(2-D)} \qquad (14)$$

for $D < 2$, and L has to be replaced by the lattice spacing a_0 for $D > 2$. In deriving (14) we implicitly assumed $\xi_0 \ll a_0/p$ with $a_0 = 1$ for the estimate of the disorder energy in (13). In the opposite limit $\xi_0 \gg a_0/p$ perturbation theory gives for the disorder energy $\sqrt{\Delta_0 L^D}$. A useful interpolation formula for L_R is therefore

$$L_R \simeq \left(\frac{v_0(\xi_0 p + 1)}{\Delta_0\xi_0 p}\right)^{1/(2-D)}. \qquad (15)$$

For $D < 2$ the flat phase is unstable and the interface is therefore rough on scales $L > L_R$ even in the presence of the crystal potential. Since the energy cost for terraces vanishes now on length scales $L \simeq L_R$, the system is described on larger scales by an effective *elastic* Hamiltonian with a stiffness constant γ_{eff}. A rough estimate for γ_{eff} follows from balancing the elastic energy and the bare energy cost for a terrace of height $2\pi/p$ on the length scale L_R,

$$\gamma_{eff}L_R^{D-2} \approx \gamma\sqrt{v_0}L_R^{D-1}p, \qquad (16)$$

which gives $\gamma_{eff} \approx \gamma L_R/w$ [33,34]. On scales $L \gg L_R$ the hump height scales as $p\phi \simeq 2\pi(L/L_R)^\zeta$ where $\zeta = (4 - D)/3$ is the roughness exponent for random fields [24,25]. L_R is physically meaningful only if it is larger than the bare kink width, $L_R > w$. This condition can be rewritten as

$$v_0 > v_{0,c} \approx \left(\frac{\Delta_0\xi_0 p^{D-1}}{1 + \xi_0 p}\right)^{2/(4-D)}. \qquad (17)$$

If $v_0 \to v_{0,c}+$, γ_{eff} changes into γ. For $v_0 < v_{0,c}$, the lattice potential can be neglected and v_0 has to be replaced by $v_{0,c}$ in the above formulas.

So far we have considered the case $D < 2$. For $D = 2$ the length scale L_R can be obtained from an argument which has been originally applied by Morgenstern *et al.* [40] and Binder [26] to the surface of an Imry-Ma domain in the two-dimensional random field Ising model. Consider again a terrace of height $2\pi/p$ and size L in the otherwise planar interface. As can be seen from equation (13), both the step energy and the random energy scale proportional to L. To calculate L_R one has to consider the distribution of random energies E_{dis} of such a terraces resulting from different disorder configurations. The mean value of this random energies vanishes, but its variance increases with L. For large enough terraces, the distribution for E_{dis} becomes Gaussian,

$$\mathcal{P}(E_{dis}) = \frac{1}{4\pi L\sqrt{\Delta_0\xi_0/p}}\exp\left(-\frac{1}{2}\frac{E_{dis}^2}{8\pi L^2\Delta_0\xi_0/p}\right). \qquad (18)$$

Since the total energy cost for a terrace of circular shape is given by the sum of the elastic energy $E_{el} = 2\pi^2\sqrt{v_0}L/p$ and E_{dis}, the probability $\mathcal{P}_<$ that the total energy becomes negative can be easily estimated to be

$$\mathcal{P}_< = \int_{-\infty}^{-E_{el}} dE_{dis}\, \mathcal{P}(E_{dis}). \qquad (19)$$

This integral evaluated in the limit $\Delta \to 0$ gives

$$\mathcal{P}_< \approx \frac{1}{\pi^2}\sqrt{\frac{p\xi_0\Delta_0}{v_0}}\exp\left(-\frac{\pi^3}{4}\frac{v_0}{p\xi_0\Delta_0}\right). \qquad (20)$$

Hence the density $\mathcal{P}_< \approx (L_R)^{-2}$ of such terraces tends exponentially to zero as $\Delta_0 \to 0$. Neglecting algebraic factors, terraces of arbitrary size appear spontaneously beyond the exponentially large length scale

$$L_R \simeq \exp\left(\frac{\pi^3}{8}\frac{v_0}{p\xi_0\Delta_0}\right) \qquad (21)$$

such that the interface becomes asymptotically rough. Thus, the flat phase is unstable to a weak random field in $D \le 2$ dimensions.

For $D > 2$, we have to expect from the previous considerations that the interface becomes rough only for $v_0 < v_{0,c}$, *i.e.*, that there is a RT as a function of v_0 (or Δ_0) at $v_0 \simeq v_{0,c}$. Since one could object that the argument for the occurrence of a critical value $v_{0,c}$ for v_0 is restricted to $D \le 2$, we give here an additional argument for the existence of a roughening transition for $D > 2$ by comparing the pinning forces which originate from the periodic and the impurity potential, respectively. If there is no disorder, an external force (density) has to overcome a threshold value

$$f_v \approx p\gamma v_0 \qquad (22)$$

to depin the interface. On the other hand, for $v_0 = 0$ the threshold force from the impurity potential on a length scale L is given by [41]

$$f_\Delta(L) \approx \gamma\xi_0 L_\Delta^\zeta L^{\zeta-2} \qquad (23)$$

where we introduced the Larkin–Fukuyama–Lee length $L_\Delta \approx (\xi_0^2/\Delta_0)^{1/(4-D)}$ and the roughening exponent ζ of the manifold in the absence of lattice pinning. The transition between the lattice pinned flat and the impurity pinned rough phase occurs if both force densities are equal on the length scale of the step width w. This gives

$$v_{0,c} \approx p^{-2}(p\xi_0)^{2/\zeta}(\Delta_0/\xi_0^2)^{2/(4-D)}. \qquad (24)$$

For random field systems, $\zeta = (4 - D)/3$ if $p\xi_0 \ll 1$ (asymptotic regime) and $\zeta = (4 - D)/2$ if $p\xi_0 \gg 1$ (perturbative regime), in complete agreement with (17).

For completeness we additionally show the stability of the rough phase to a weak crystal potential. Indeed, lowest order perturbation theory in v_0 yields an effective Hamiltonian where the periodic crystal potential is replaced by a mass term $m^2\phi^2/2$. Assuming a Gaussian distributed field $\phi(\mathbf{x})$, which is justified to lowest order in $\epsilon = 4 - D$, we obtain on length scales $L > L_\Delta$ for the mass

$$m^2 = p^2 v_0\overline{\cos(p\phi)} = p^2 v_0 \exp[-p^2\overline{\phi^2}/2]$$
$$= p^2 v_0 \exp[-2\pi^2(L/L_\Delta)^{2\zeta}]. \qquad (25)$$

Comparing this exponential behavior in L with the $L^{2\zeta-2}$ scaling of the elastic energy, we conclude that the perturbation is always irrelevant since $\zeta > 0$ for the elastic

manifold models. Likewise, the flat phase is stable to a weak random potential as can be shown easily by perturbation theory with respect to V_R. From the stability of both phases in $D > 2$ dimensions we can expect that there is a roughening transition for $D > 2$ as a function of v_0 (or Δ_0) at $v_0 \simeq v_{0,c}(\Delta_0)$.

In the rough phase, the mean square displacement of the interface can be estimated again from the energy

$$\frac{E_{total}}{\gamma L^{D-2}} \simeq \phi^2 + \sqrt{v_0} L \phi e^{-p^2\phi^2/2} - \sqrt{\xi_0 \Delta_0 \phi} L^{(4-D)/2}. \tag{26}$$

Here we have included both the elastic and the step energy term to describe the crossover from $v_0 \ll v_{0,c}$ to $v_0 \simeq v_c$. Moreover, we have treated the lattice pinning term in a self consistent harmonic approximation to account for a situation in which $p\phi \gtrsim 2\pi$. In the rough phase, the hump height asymptotically scales with the roughness exponent $\zeta = (4 - D)/3$ as a result of the balance between the first and the last term in equation (26). However, there is an intermediate length scale region up to $\xi_\parallel$ in which the roughness of the interface is dominated by the competition between the second and the last term of equation (26). In this region the roughness increases only logarithmically,

$$\overline{\phi^2} \approx \frac{2}{p^2}(D-2)\ln\left(\frac{L}{L_R}\right). \tag{27}$$

This result will be confirmed below by the RG calculation which yields also the exponent $\nu_\parallel$ of the crossover length $\xi_\parallel$ to first order in $\epsilon = 4 - D$. Finally, for $v_0 \gg v_{0,c}$ the interface is always flat.

So far we have treated only the case of random fields. For *random bond systems* similar arguments apply but the asymptotic roughness cannot be obtained correctly from a Flory argument.

For *periodic elastic media*, arguments identical to those used before for manifolds give a lower critical dimension $D_c(= d_c) = 2$ for the occurrence of a roughening transition and the estimate (17) for the critical value of $v_{0,c}$ if we set $\xi_0 p \gg 1$.

To estimate the influence of a weak crystal potential in the rough phase, we compare again the scaling of the elastic energy with that of the effective mass m^2 as given by equation (25). In what follows, the logarithmic roughness of the structure, $\overline{\phi^2} = \frac{\pi^2}{9}(4-D)\ln(L/L_\Delta)$, on length scales $L > L_\Delta$ and for $2 < D < 4$, *cf.* Section 5, is crucial. Due to this weak roughness, the effective mass decays only algebraically on large length scales L,

$$m^2 = p^2 v_0 \left(\frac{L}{L_\Delta}\right)^{-\pi^2 p^2(4-D)/18}. \tag{28}$$

The elastic energy simply scales as L^{-2} and thus we conclude that the crystal potential is a relevant perturbation if

$$p < p_c \equiv \frac{6}{\pi\sqrt{4-D}} \tag{29}$$

leading always to a flat phase. For $p > p_c$ the rough phase is again stable and one has to expect a roughening transition. Possible subtleties about exchanging the limits of large L and small ϵ have been neglected here, but this result will be reproduced below by a detailed RG double expansion in $\epsilon = 4 - D$ and $\mu = p^2/p_c^2 - 1$.

So far we have neglected thermal fluctuations. In $D > 2$, where we have anticipated the occurrence of a roughening transition, thermal fluctuations are irrelevant. In $D \leq 2$ fluctuations are still dominated by disorder fluctuations on large scales. However, for weak disorder and sufficiently high temperatures $T > T_R$, a length cross-over from thermal to disorder dominated pinning phenomena will occur as briefly discussed in [33,34].

4 Functional renormalization group

Next we employ a functional RG calculation, which starts with the disorder averaged replica-Hamiltonian (5). We apply a momentum shell RG to this Hamiltonian, in which the high-momentum modes of $\phi(\mathbf{x})$ in a shell of infinitesimal width, $|\mathbf{q}| \in [\Lambda e^{-dl}, \Lambda]$, are integrated out. The momentum cutoff Λ will be kept fixed by rescaling coordinates and fields according to

$$\mathbf{x} = e^{dl}\mathbf{x}', \quad \phi(\mathbf{x}) = e^{\zeta dl}\phi'(\mathbf{x}'). \tag{30}$$

Since the behavior of the elastic objects should be described by zero-temperature fixed points, we allow the temperature to be renormalized by keeping the elastic stiffness constant γ fixed. From the above scale changes we obtain the RG flow of the temperature,

$$\frac{dT}{dl} = (2 - D - 2\zeta)T. \tag{31}$$

It can be shown that this flow equation is exact for vanishing lattice potential due to the tilt symmetry of the Hamiltonian (1) for $V_L(\phi) = 0$ [42]. As we will see below, a finite lattice potential leads to a renormalization of the elastic stiffness which can be rewritten as a renormalization of the temperature. This leads to an additional term in equation (31) but does *not* change the temperature into a relevant RG variable.

The RG equations for $V_L(\phi)$ and $R(\phi)$ will be derived in their functional form following the method developed by Balents and Fisher [43]. The two last terms of the replica-Hamiltonian (5) will be considered as a small perturbation $\mathcal{H}_{pert}$ of the elastic gradient term which we denote by $\mathcal{H}_0$. To eliminate the high-momentum modes, the field is divided into slowly and rapidly varying contributions, $\phi(\mathbf{x}) = \phi^<(\mathbf{x}) + \phi^>(\mathbf{x})$. The feedback from integrating out $\phi^>(\mathbf{x})$ can be calculated by expanding the effective replica-Hamiltonian for the slow fields $\phi^<(\mathbf{x})$,

$$\tilde{\mathcal{H}}_n = -\ln\int[d\phi_\alpha^>]\exp(-\mathcal{H}_n), \tag{32}$$

in powers of $\mathcal{H}_{pert}$. The first terms of this cumulant expansion are given by

$$\tilde{\mathcal{H}}_n = \mathcal{H}_0 + \langle \mathcal{H}_{pert} \rangle_{>,c} - \frac{1}{2} \langle \mathcal{H}_{pert}^2 \rangle_{>,c} + \frac{1}{6} \langle \mathcal{H}_{pert}^3 \rangle_{>,c} - \cdots \tag{33}$$

Here $\langle \ldots \rangle_{>,c}$ denotes the connected expectation value over $\phi^>(\mathbf{x})$ with respect to $\mathcal{H}_0$. Generally, new interactions which are not present in the original Hamiltonian are generated by the RG transformation and have to be included in $\mathcal{H}_{pert}$ if they are relevant in the RG sense. We postpone the discussion of such sort of terms to the step in the RG calculation where they appear for the first time.

Now we start to evaluate the series (33) order by order. To obtain the feedback of *first order* from the perturbation, we rewrite $\mathcal{H}_{pert}$ in its Fourier representation,

$$-\mathcal{H}_{pert} = \frac{1}{2T^2} \sum_{\alpha\beta} \int_{\mathbf{x},\mathbf{k}} e^{i\mathbf{k}\phi_{\alpha\beta}(\mathbf{x})} \tilde{R}(\mathbf{k})$$
$$+ \frac{1}{T} \sum_{\alpha} \int_{\mathbf{x},\mathbf{k}} e^{i\mathbf{k}\phi_{\alpha}(\mathbf{x})} \tilde{V}_L(\mathbf{k}), \tag{34}$$

where we use here and in the following the vector $\mathbf{k}$ for Fourier transforms with respect to ϕ, whereas the vector $\mathbf{q}$ will be used to denote momenta in $\mathbf{x}$ direction. Furthermore, we have introduced the abbreviations $\int_{\mathbf{x},\mathbf{k}} \equiv \int d^D\mathbf{x} \int d^N\mathbf{k}/(2\pi)^N$, $\phi_{\alpha\beta}(\mathbf{x}) \equiv \phi_\alpha(\mathbf{x}) - \phi_\beta(\mathbf{x})$ and $\gamma/T \to 1/T$.

After decomposition into slow and rapid fields, the average over the fast modes in equation (34) can be easily performed using Wick's theorem. For simplicity, we will drop the label $<$ on the slow fields in the averaged expressions,

$$-\langle \mathcal{H}_{pert} \rangle_{>,c}$$
$$= \frac{1}{2T^2} \sum_{\alpha\beta} \int_{\mathbf{x},\mathbf{k}} e^{i\mathbf{k}\phi_{\alpha\beta}(\mathbf{x})} e^{-\mathbf{k}^2 T G_>(\mathbf{0})(1-\delta_{\alpha\beta})} \tilde{R}(\mathbf{k})$$
$$+ \frac{1}{T} \sum_{\alpha} \int_{\mathbf{x},\mathbf{k}} e^{i\mathbf{k}\phi_{\alpha}(\mathbf{x})} e^{-\frac{1}{2}\mathbf{k}^2 T G_>(\mathbf{0})} \tilde{V}_L(\mathbf{k}). \tag{35}$$

Here we have introduced the free two-point function

$$G_>(\mathbf{x}) = \int_{\mathbf{q}}^> \frac{e^{i\mathbf{q}\mathbf{x}}}{\mathbf{q}^2} \equiv \int\limits_{|\mathbf{q}|=\Lambda e^{-dl}}^{\Lambda} \frac{d^D\mathbf{q}}{(2\pi)^D} \frac{e^{i\mathbf{q}\mathbf{x}}}{\mathbf{q}^2}, \tag{36}$$

where the label $>$ on the integral denotes integration over the infinitesimal momentum shell. In the limit $dl \to 0$ this function, at $\mathbf{x} = \mathbf{0}$, becomes

$$G_>(\mathbf{0}) = (2\pi)^{-D} S_D \Lambda^{D-2} dl \equiv K_D \Lambda^{D-2} dl, \tag{37}$$

where S_D is the surface area of a unit sphere in D dimensions. Since we have to calculate the expectation value of the perturbation to first order in dl, the exponentials in equation (35) depending on the two-point function $G_>(\mathbf{0})$

Fig. 2. Diagrams arising in first order of the cumulant expansion. The closed lines represent $G_>(\mathbf{0})$. Both diagrams contribute to the free energy only, see equation (38).

can be expanded with respect to dl. This yields

$$-\langle \mathcal{H}_{pert} \rangle_{>,c}$$
$$= \frac{1}{2T^2} \sum_{\alpha\beta} \int_{\mathbf{x}} R(\phi_{\alpha\beta}) + \frac{1}{T} \sum_{\alpha} \int_{\mathbf{x}} V_L(\phi_{\alpha})$$
$$+ \frac{K_D \Lambda^{D-2} dl}{2T} \int_{\mathbf{x}} \left\{ \sum_{\alpha\beta} \partial_i \partial_i R(\phi_{\alpha\beta}) - n \partial_i \partial_i R(\mathbf{0}) \right\}$$
$$+ \frac{K_D \Lambda^{D-2} dl}{2} \int_{\mathbf{x}} \sum_{\alpha} \partial_i \partial_i V_L(\phi_{\alpha}). \tag{38}$$

The corresponding diagrams are shown in Figure 2. Here and below the partial derivatives ∂_i act on the field ϕ, and repeated Latin indices are summed over from 1 to N. Whereas the first two terms are simply the original perturbation, the remaining new parts are generated by the RG. The first and the last term of this new part is of the appropriate form to renormalize $R(\phi)$ and $V_L(\phi)$ but they are reduced by a factor of T compared to the original ones. Thus they are irrelevant at the zero temperature fixed points. The second new term proportional to n contributes only to the renormalization of the free energy. Therefore we conclude that in first order of the cumulant expansion there is no renormalization of $R(\phi)$ or $V_L(\phi)$.

Now we turn to the analysis of the *second order* contributions to the renormalized Hamiltonian. Averaging over the fields $\phi^>$, this contribution becomes

$$\frac{1}{2} \langle \mathcal{H}_{pert}^2 \rangle_{>,c}$$
$$= \int_{\substack{\mathbf{x}_1,\mathbf{k}_1 \\ \mathbf{x}_2,\mathbf{k}_2}} \left\{ \frac{1}{8T^4} \sum_{\substack{\alpha_1\beta_1 \\ \alpha_2\beta_2}} e^{i\mathbf{k}_1\phi_{\alpha_1\beta_1}(\mathbf{x}_1) + i\mathbf{k}_2\phi_{\alpha_2\beta_2}(\mathbf{x}_2)} \right.$$
$$\times e^{-\mathbf{k}_1^2 T G_>(\mathbf{0})(1-\delta_{\alpha_1\beta_1}) - \mathbf{k}_2^2 T G_>(\mathbf{0})(1-\delta_{\alpha_2\beta_2})}$$
$$\times e^{-\mathbf{k}_1\mathbf{k}_2 T G_>(\mathbf{x}_1-\mathbf{x}_2)(\delta_{\alpha_1\alpha_2} + \delta_{\beta_2\beta_2} - \delta_{\alpha_1\beta_2} - \delta_{\beta_1\alpha_2})} \tilde{R}(\mathbf{k}_1) \tilde{R}(\mathbf{k}_2)$$
$$+ \frac{1}{2T^3} \sum_{\substack{\alpha_1\beta \\ \alpha_2}} e^{i\mathbf{k}_1\phi_{\alpha_1\beta_1}(\mathbf{x}_1) + i\mathbf{k}_2\phi_{\alpha_2}(\mathbf{x}_2)} e^{-\mathbf{k}_1^2 T G_>(\mathbf{0})(1-\delta_{\alpha_1\beta})}$$
$$\times e^{-\frac{1}{2}\mathbf{k}_2^2 T G_>(\mathbf{0})} e^{-\mathbf{k}_1\mathbf{k}_2 T G_>(\mathbf{x}_1-\mathbf{x}_2)(\delta_{\alpha_1\alpha_2} - \delta_{\beta\alpha_2})} \tilde{R}(\mathbf{k}_1) \tilde{V}_L(\mathbf{k}_2)$$
$$+ \frac{1}{2T^2} \sum_{\alpha_1\alpha_2} e^{i\mathbf{k}_1\phi_{\alpha_1}(\mathbf{x}_1) + i\mathbf{k}_2\phi_{\alpha_2}(\mathbf{x}_2)} e^{-\frac{1}{2}(\mathbf{k}_1^2+\mathbf{k}_2^2) T G_>(\mathbf{0})}$$
$$\left. \times e^{-\mathbf{k}_1\mathbf{k}_2 T G_>(\mathbf{x}_1-\mathbf{x}_2)\delta_{\alpha_1\alpha_2}} \tilde{V}_L(\mathbf{k}_1) \tilde{V}_L(\mathbf{k}_2) \right\} - \text{d.t.}, \tag{39}$$

where d.t. stands for disconnected terms which have to be subtracted from the above expression. To obtain the contributions to first order in dl, we have to expand the exponentials depending on $G_>$ up to second order in T.
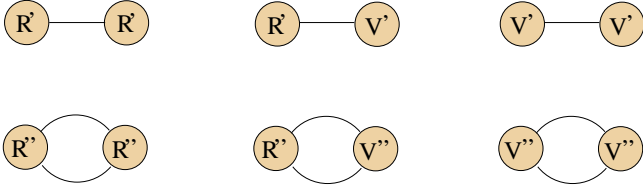
Fig. 3. Diagrams arising in second order of the cumulant expansion, where the internal lines represent $G_>(\mathbf{x} - \mathbf{x}')$. The graphs with one internal line contribute only at large momenta and can be neglected.

Sorting out the disconnected parts, the terms proportional to $G_>(\mathbf{0})$ are canceled. Performing the summation over the replica indices and transforming back to real space, we obtain the following second order result,

$$
\begin{aligned}
&\frac{1}{2}\langle \mathcal{H}_{pert}^2 \rangle_{>,c} \\
&= \int_{\mathbf{x},\mathbf{x}'} \left\{ \frac{1}{2T^3} \sum_{\alpha\beta\gamma} \partial_i R(\phi_{\alpha\beta}(\mathbf{x}))\partial_i R(\phi_{\alpha\gamma}(\mathbf{x}')) \right. \\
&\quad + \frac{1}{T^2} \sum_{\alpha\beta} \partial_i R(\phi_{\alpha\beta}(\mathbf{x}))\partial_i V_L(\phi_{\alpha}(\mathbf{x}')) \\
&\quad \left. + \frac{1}{2T} \sum_{\alpha} \partial_i V_L(\phi_{\alpha}(\mathbf{x}))\partial_i V_L(\phi_{\alpha}(\mathbf{x}')) \right\} G_>(\mathbf{x} - \mathbf{x}') \\
&\quad + \int_{\mathbf{x},\mathbf{x}'} \left\{ \frac{1}{4T^2} \sum_{\alpha\beta\gamma} \partial_i\partial_j R(\phi_{\alpha\beta}(\mathbf{x}))\partial_i\partial_j R(\phi_{\alpha\gamma}(\mathbf{x}')) \right. \\
&\quad + \frac{1}{4T^2} \sum_{\alpha\beta} \left[\partial_i\partial_j R(\phi_{\alpha\beta}(\mathbf{x}))\partial_i\partial_j R(\phi_{\alpha\beta}(\mathbf{x}')) \right. \\
&\quad \left. - 2\partial_i\partial_j R(\phi_{\alpha\beta}(\mathbf{x}))\partial_i\partial_j R(\mathbf{0}) \right] \\
&\quad - \frac{1}{2T} \sum_{\alpha} \partial_i\partial_j R(\mathbf{0})\partial_i\partial_j V_L(\phi_{\alpha}(\mathbf{x}')) \\
&\quad \left. + \frac{1}{4} \sum_{\alpha} \partial_i\partial_j V_L(\phi_{\alpha}(\mathbf{x}))\partial_i\partial_j V_L(\phi_{\alpha}(\mathbf{x}')) \right\} G_>^2(\mathbf{x} - \mathbf{x}')
\end{aligned}
$$
$$(40)$$

corresponding to the diagrams in Figure 3. The three terms within the first curly bracket have a contribution only at large momenta since $G_>(\mathbf{x})$ is composed only of momenta within the shell. The first of these contributions is a 3-replica term which does not fit into the form of the original replica-Hamiltonian (5). Such terms with more than two replicas result from non-Gaussian correlations in the disorder and are generated by the RG. Anticipating that $R(\phi)$ will be of order ϵ at the fixed points, the renormalization of $R(\phi)$ and $V_L(\phi)$ resulting from 3-replica parts will be of higher order in ϵ since the 3-replica terms are generated only at large momenta. Similarly, one can argue that also the other two large momenta terms in the first curly bracket do not influence the RG results to lowest order in the small parameters of the RG expansion. Note that it may become necessary to introduce a second small parameter which controls the fixed point value of the lattice potential $V_L(\phi)$. Therefore, we will drop in the

following all terms generated by the RG which contribute only at large momenta.

From the terms in the second curly brackets, the first one which has three replica indices would renormalize terms with three replicas which would appear in the original Hamiltonian with a temperature dependence $\sim T^{-3}$ such that the above term can be neglected at a $T = 0$ fixed point. The next two terms are relevant and lead to a renormalization of $R(\phi)$ and $V_L(\phi)$, respectively. The last term is also of the right form to feed back into $V_L(\phi)$, but it is down by a factor of T and hence negligible.

To evaluate the two relevant contributions of equation (40), we note that main contribution to the $\mathbf{x}'$-integration comes from $\mathbf{x}' = \mathbf{x}$ since $G_>(\mathbf{x} - \mathbf{x}')$ then becomes maximal. Therefore, we make of change of coordinates according to $\mathbf{x}' \to \mathbf{x} + \mathbf{x}'$ and expand the interactions with respect to $\mathbf{x}'$. This gives formally expressions of the form

$$
\begin{aligned}
&\int_{\mathbf{x},\mathbf{x}'} F(\mathbf{x})F(\mathbf{x}')G_>^2(\mathbf{x} - \mathbf{x}') = \int_{\mathbf{x},\mathbf{x}'} F(\mathbf{x})F(\mathbf{x}+\mathbf{x}')G_>^2(\mathbf{x}') \\
&= \int_{\mathbf{x}} F^2(\mathbf{x}) \int_{\mathbf{x}'} G_>^2(\mathbf{x}') + \int_{\mathbf{x}} F(\mathbf{x})\boldsymbol{\nabla}F(\mathbf{x}) \cdot \int_{\mathbf{x}'} \mathbf{x}'G_>^2(\mathbf{x}') \\
&\quad + \int_{\mathbf{x}} \frac{1}{2}F(\mathbf{x})\partial_{\mathbf{x}_n}\partial_{\mathbf{x}_m}F(\mathbf{x}) \int_{\mathbf{x}'} \mathbf{x}'_n\mathbf{x}'_m G_>^2(\mathbf{x}') + \mathcal{O}(\mathbf{x}'^3), (41)
\end{aligned}
$$

where n and m are summed over from 1 to D. The part which is linear in $\mathbf{x}'$ vanishes due to the symmetry of $G_>(\mathbf{x}')$. Since $G_>(\mathbf{x})$ is composed only of momenta of the shell, the kernel $G_>^2(\mathbf{x})$ can be easily integrated to first order in dl,

$$
\int_{\mathbf{x}} G_>^2(\mathbf{x}) = K_D \Lambda^{D-4} dl. \tag{42}
$$

Generally, one may expect also the appearance of quadratic gradient terms from second derivatives of $F(\mathbf{x})$ in the above expansion, resulting in a renormalization of the elastic stiffness constant γ. Whereas the absence of any V_L terms in the relevant contributions $\sim R^2$ renders gradient terms strongly irrelevant, they have to be taken into account for the RV_L part. Up to second order in $\boldsymbol{\nabla}\phi$, the non-vanishing parts of a gradient expansion of the penultimate term of equation (40) are

$$
\begin{aligned}
&- \frac{1}{2T} \sum_{\alpha} \int_{\mathbf{x},\mathbf{x}'} \partial_i\partial_j R(\mathbf{0})\left\{ \partial_i\partial_j V_L(\phi_{\alpha}(\mathbf{x})) \right. \\
&\quad \left. + \frac{1}{2}\partial_i\partial_j\partial_k\partial_l V_L(\phi_{\alpha}(\mathbf{x}))\mathbf{x}'\boldsymbol{\nabla}\phi_{\alpha}^k(\mathbf{x}) \cdot \mathbf{x}'\boldsymbol{\nabla}\phi_{\alpha}^l(\mathbf{x}) \right\} G_>^2(\mathbf{x}').
\end{aligned}
$$
$$(43)$$

The first term contributes to the renormalization of V_L whereas from the last part one may expect a change of the elastic stiffness. Thus to lowest order in the gradient expansion, we end up with the following contributions,

$$
\begin{aligned}
\delta^{(2)} R &= \frac{1}{2}K_D\Lambda^{D-4}dl \left\{ \partial_i\partial_j R(\phi)\partial_i\partial_j R(\phi) \right. \\
&\quad \left. - 2\partial_i\partial_j R(\phi)\partial_i\partial_j R(\mathbf{0}) \right\} \\
\delta^{(2)} V_L &= -\frac{1}{2}K_D\Lambda^{D-4}dl\,\partial_i\partial_j R(\mathbf{0})\partial_i\partial_j V_L(\phi), \quad (44)
\end{aligned}
$$

where $\delta^{(n)}R$ and $\delta^{(n)}V_L$ denote here and in the following the nth cumulant order feedback to the renormalization of $R(\boldsymbol{\phi})$ and $V_L(\boldsymbol{\phi})$, respectively.

To analyze the last term in equation (43) we note that $\partial_i\partial_j V_L(\boldsymbol{\phi}) \sim \delta_{ij}$ since we have assumed the particularly simple form (2) for the lattice potential. Therefore the diagonal structure of the elastic kernel is preserved. To obtain the relevant contribution to the stiffness constant γ, the gradient term has to be expanded in terms of eigenfunctions of the linear operator of the RG flow of $V_L(\boldsymbol{\phi})$ [44]. This linear operator is given by

$$\mathcal{L}V_L = (2 - 2\zeta)V_L + \zeta\phi^i\partial_i V_L - \frac{1}{2}\partial_i\partial_j R(\mathbf{0})\partial_i\partial_j V_L, \quad (45)$$

where the last term stems from the second order contribution (44) and the remaining parts arise from rescaling. The determination of eigenfunctions is simple since $\partial_i\partial_j R(\mathbf{0}) = -\delta_{ij}\Delta$ in all cases of interest. It is simple to see that the eigenfunctions are given by

$$E_{\mathbf{m}}(\boldsymbol{\phi}) = \cos(pm_1\phi^1) \cdot \ldots \cdot \cos(pm_N\phi^N) \quad (46)$$

with $\mathbf{m} = (m_1, \ldots, m_N)$ a vector of integers. Here we have taken into account the rescaling of $\boldsymbol{\phi}(\mathbf{x})$ by allowing for a periodicity a of the lattice potential which depends on the flow parameter l such that $da/dl = -\zeta a$. Then the eigenfunctions multiplied by the simple exponential factor $\exp(\lambda_{\mathbf{m}}l)$ are solutions of the linear RG flow $dV_L/dl = \mathcal{L}V_L$. The scaling dimension of this eigenfunctions at a fixed point is given by the corresponding eigenvalues

$$\lambda_{\mathbf{m}} = 2 - 2\zeta - \frac{1}{2}\mathbf{m}^2 \lim_{l\to\infty} p^2\Delta. \quad (47)$$

It will turn out below that at these fixed points, where the lattice potential $V_L(\boldsymbol{\phi})$ has a finite value, the eigenvalues become $\lambda_{\mathbf{m}} = 2(1 - \mathbf{m}^2)$ up to corrections of the order of the small parameters of the RG expansion, $e.g.$ ϵ. Therefore, we see that higher harmonics of the lattice potential with $\mathbf{m}^2 > 1$ are strongly irrelevant for the large scale behavior of the elastic object. This justifies the assumption of equation (2) for the lattice potential.

To analyze the last term of equation (43), this term has to be written as a linear combination of the operators

$$K_{\mathbf{m}} = \frac{1}{T}\int_{\mathbf{x}} E_{\mathbf{m}}(\boldsymbol{\phi})\boldsymbol{\nabla}\boldsymbol{\phi}\cdot\boldsymbol{\nabla}\boldsymbol{\phi}. \quad (48)$$

For $\mathbf{m}^2 > 0$, all these operators are strongly irrelevant with scaling dimensions $\lambda_{\mathbf{m}} - 2 + 2\zeta$ at the fixed points with finite lattice potential. Therefore only the projection of the gradient term in equation (43) onto the constant eigenfunction $E_{\mathbf{0}}(\boldsymbol{\phi})$ can potentially contribute to the renormalization of the stiffness constant. But this projection vanishes since $V_L(\boldsymbol{\phi})$ is simply a sum of first harmonics. Thus γ is not renormalized to first order in the lattice potential, and we have no contribution to γ from second cumulant order,

$$\delta^{(2)}\gamma = 0 \quad (49)$$

where $\delta^{(n)}$ denotes the nth order feedback to γ.

To obtain a finite fixed point for $V_L(\boldsymbol{\phi})$, we have to calculate the RG flow up to the first non-vanishing non-linear order in $V_L(\boldsymbol{\phi})$. Therefore, we have to consider now contributions from $third\ order$ of $\mathcal{H}_{pert}$. In this order only terms of the order RV_L^2 are relevant as will be explained now. The terms $\sim R^3$ generate only three-replica parts which will be of order ϵ^2 and can therefore be neglected. On the other hand, the contributions $\sim V_L^3$ which would be able to renormalize V_L are reduced by a factor of T and thus are also negligible at the zero-temperature fixed point. For the terms of the order R^2V_L the discussion is slightly more complicated. The corresponding two-replica terms generated in this order are of the form

$$\frac{1}{T^2}\int_{\mathbf{x}}\sum_{\alpha\beta}\partial_i\partial_j R(\boldsymbol{\phi}_{\alpha\beta})\partial_i\partial_k R(\boldsymbol{\phi}_{\alpha\beta})\partial_j\partial_k V_L(\boldsymbol{\phi}_\alpha), \quad (50)$$

which does not fit into the form of the terms present in the original Hamiltonian. To analyze this unusual term, one has to expand again the lattice potential $V_L(\boldsymbol{\phi})$ into eigenfunctions of the linear operator of the RG flow equation for $V_L(\boldsymbol{\phi})$. This will enable us to determine the relevance of contributions of the form (50). For that purpose we rewrite (50) as a linear combination of operators defined by

$$S_{\mathbf{m}} = \frac{1}{T^2}\int_{\mathbf{x}}\sum_{\alpha\beta}\partial_i\partial_j R(\boldsymbol{\phi}_{\alpha\beta})\partial_i\partial_k R(\boldsymbol{\phi}_{\alpha\beta})E_{\mathbf{m}}(\boldsymbol{\phi}_\alpha). \quad (51)$$

The scaling dimension of these operators can easily be obtained in terms of $\lambda_{\mathbf{m}}$. It turns out that the operators $S_{\mathbf{m}}$ for all $\mathbf{m}$ are strongly irrelevant with scaling dimensions $-D - 2 - 2\zeta + \lambda_{\mathbf{m}} = -4 - 2\mathbf{m}^2 + \mathcal{O}(\epsilon)$. Therefore, terms of the form (50) are generated by the RG but are negligible for the large-scale behavior.

The only terms in third order remaining to be discussed are proportional to RV_L^2. In contrast to the other combinations of R and V_L treated above, these terms produce a relevant feedback to renormalize V_L. The corresponding part of $\langle\mathcal{H}_{pert}^3\rangle_{>,c}$ is given by an expression similar to those appearing in equation (39). In third order the relevant contributions come from the T^3 terms of the expansion of the exponentials containing the function $G_>(\mathbf{x})$. Integrating out the rapid modes and transforming back to real space, we end up with the result

$$\frac{1}{2T}\int_{\substack{\mathbf{x}_1 \\ \mathbf{x}_2 \\ \mathbf{x}_3}}\sum_\alpha \partial_i\partial_j R(\mathbf{0})\partial_i\partial_k V_L(\boldsymbol{\phi}(\mathbf{x}_2))\partial_j\partial_k V_L(\boldsymbol{\phi}(\mathbf{x}_3))$$
$$\times G_>(\mathbf{x}_1 - \mathbf{x}_2)G_>(\mathbf{x}_1 - \mathbf{x}_3)G_>(\mathbf{x}_2 - \mathbf{x}_3) \quad (52)$$

represented by the graph in Figure 4a. We obtain in lowest order of the gradient expansion in equation (41) the following third order contribution to $V_L(\boldsymbol{\phi})$,

$$\delta^{(3)}V_L = -\frac{1}{2}K_D\Lambda^{D-6}dl\partial_i\partial_j R(\mathbf{0})\partial_i\partial_k V_L(\boldsymbol{\phi})\partial_j\partial_k V_L(\boldsymbol{\phi}). \quad (53)$$

(a)   (b)
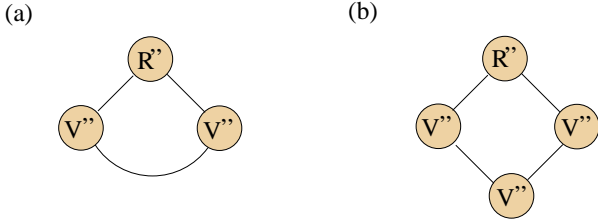
Fig. 4. Relevant graphs which appear in third (a) and fourth order (b) of the cumulant expansion. In both cases the disorder vertex contributes only a ϕ-independent factor $\partial_i\partial_j R(\mathbf{0})$.

But for this sort of feedback also higher order terms of the gradient expansion are relevant. The corresponding expression in second order in $\nabla\phi$ is given by

$$
\frac{1}{2T}\int_{\substack{\mathbf{x}_1 \\ \mathbf{x}_2 \\ \mathbf{x}_3}}\sum_{\alpha}\partial_i\partial_j R(\mathbf{0})\partial_i\partial_k\partial_l V_L(\phi_\alpha(\mathbf{x}_1))\partial_j\partial_k\partial_m V_L(\phi_\alpha(\mathbf{x}_1))
$$
$$
\times\mathbf{x}_2\nabla\phi_\alpha^l(\mathbf{x}_1)\cdot\mathbf{x}_3\nabla\phi_\alpha^m(\mathbf{x}_1)G_>(\mathbf{x}_2)G_>(\mathbf{x}_3)G_>(\mathbf{x}_2-\mathbf{x}_3).
$$
(54)

As before, the diagonal structure of the elastic part is preserved by this feedback due to $\partial_i\partial_j V_L \sim \delta_{ij}$. In contrast to the second part of equation (43), this contribution is quadratic in V_L. Therefore, also the first harmonics of the lattice potential yield a non-vanishing projection onto the constant eigenfunction $E_{\mathbf{0}}(\phi)$ since $\sin^2(p\phi) = (1-\cos(2p\phi))/2$. Performing the spatial integration over $\mathbf{x}_2$ and $\mathbf{x}_3$ to lowest order in dl and ϵ, we obtain the relevant feedback to the stiffness constant from third cumulant order,

$$
\delta^{(3)}\gamma = -K_D\Lambda^{D-8}dl\partial_i\partial_j R(\mathbf{0})
$$
$$
\times\mathcal{P}_0[\partial_i\partial_k\partial_l V_L(\phi)\partial_j\partial_k\partial_l V_L(\phi)].
$$
(55)

Here $\mathcal{P}_0$ denotes the projection operator onto the eigenfunction $E_{\mathbf{0}}(\phi)$.

Below we prefer to keep the stiffness constant fixed by allowing the temperature to flow, so we have to rewrite the feedback (55) as a renormalization of T. But this means that also the feedback to the functions $R(\phi)$ and $V_L(\phi)$ is changed due to the overall factor $1/T$ in front of the Hamiltonian. The effective but non-rescaled quantities are then given to first order in dl by

$$
T_{eff} = (1-\delta^{(3)}\gamma)T, \tag{56}
$$
$$
R_{eff} = (1-2\delta^{(3)}\gamma)R + \delta^{(2)}R, \tag{57}
$$
$$
V_{L,eff} = (1-\delta^{(3)}\gamma)V_L + \delta^{(2)}V_L + \delta^{(3)}V_L. \tag{58}
$$

The part $\delta^{(3)}\gamma$ is quadratic in V_L, and it is tempting to neglect this term in equation (58) since it produces cubic V_L terms which appear irrelevant compared to the term $\delta^{(3)}V_L$ which is quadratic in V_L. But it turns out that this quadratic term does not contribute to the RG flow of the first and only relevant harmonics of the lattice potential. The reason for this is that a squared first harmonic produces only a constant and a second order harmonic after projecting onto the eigenfunctions $E_{\mathbf{m}}(\phi)$.

As explained above, the lowest non-linear V_L term in the flow equation of V_L will be of third order. Since all relevant contributions have to include at least one disorder vertex $\sim R$, we have to consider also possible feedback to V_L from the *fourth order* cumulant. Simple counting of the R and V_L orders suggests that in this order terms proportional to $R^2V_L^2$ and RV_L^3 have to be taken into account. For the first type of feedback similar arguments as those for the contribution of equation (50) show that it is irrelevant in the RG sense. In contrast, the second kind of terms generates a relevant renormalization of V_L. This feedback can again be calculated along the lines described above. Now the relevant connected low-momenta parts come from the T^4 terms of the expansion of the exponentials with respect to the two-point function $G_>(\mathbf{x})$. To first order in dl the 4th order contribution becomes

$$
\delta^{(4)}V_L = -\frac{1}{2}K_D\Lambda^{D-8}dl\partial_i\partial_j R(\mathbf{0})\partial_i\partial_k V_L(\phi)\partial_j\partial_m V_L(\phi)
$$
$$
\times\partial_k\partial_m V_L(\phi).
$$
(59)

This part follows from the lowest order of the gradient expansion in equation (41); higher gradient terms are irrelevant since they could lead to a renormalization of γ only of third order in V_L and, therefore, could produce higher order terms only in the flow equation for V_L. Therefore contributions to γ of higher than second order in V_L can be neglected.

Moreover, it is important to note that in higher than fourth order of the cumulant expansion no relevant terms are generated which renormalize R and V_L to lowest non-linear order. For example, in fifth order terms appear which are cubic in V_L and of the right form to renormalize V_L but with a coefficient proportional to R^2. Therefore we can stop our analysis in fourth order of the cumulant expansion.

Keeping track of all relevant feedbacks calculated above and introducing the function

$$
W(\phi) = \partial_i\partial_j R(\mathbf{0})\partial_i\partial_k\partial_m V_L(\phi)\partial_j\partial_k\partial_m V_L(\phi), \tag{60}
$$

we obtain the resulting functional RG equations, valid to lowest order in $\epsilon = 4 - D$,

$$
\frac{dT}{dl} = (2 - D - 2\zeta + \mathcal{P}_0[W(\phi)])T \equiv -\theta T, \tag{61}
$$
$$
\frac{dR(\phi)}{dl} = (4 - D - 4\zeta)R(\phi) + \zeta\phi^i\partial_i R(\phi)
$$
$$
+ \frac{1}{2}\partial_i\partial_j R(\phi)\partial_i\partial_j R(\phi) - \partial_i\partial_j R(\mathbf{0})\partial_i\partial_j R(\phi)
$$
$$
+ 2\mathcal{P}_0[W(\phi)]R(\phi), \tag{62}
$$
$$
\frac{dV_L(\phi)}{dl} = (2 - 2\zeta)V_L(\phi) + \zeta\phi^i\partial_i V_L(\phi)
$$
$$
- \frac{1}{2}\partial_i\partial_j R(\mathbf{0})[\partial_i\partial_j V_L(\phi)+\partial_i\partial_k V_L(\phi)\partial_j\partial_k V_L(\phi)
$$
$$
+ \partial_i\partial_k V_L(\phi)\partial_j\partial_m V_L(\phi)\partial_k\partial_m V_L(\phi)]
$$
$$
+ \mathcal{P}_0[W(\phi)]V_L(\phi), \tag{63}
$$

where we made the replacements $\Lambda^{-2}V_L(\phi) \to V_L(\phi)$, $K_D\Lambda^{D-4}R(\phi) \to R(\phi)$ with $K_D^{-1} = 2^{D-1}\pi^{D/2}\Gamma(D/2)$.

5 Absence of lattice pinning: the rough phase

Much is known about the equilibrium behavior of elastic manifolds and periodic elastic media embedded in a disordered background for D just below the upper critical dimension four. In the following, we will briefly summarize the known results for the roughness exponent ζ in the various cases. In addition, we will develop a simplified calculation scheme to obtain the effective disorder strength or, equivalently, the RG flow of the disorder potential on sufficiently large but finite length scales. This technique becomes useful if we study the competition between random and crystal pinning in Section 6.

In the absence of lattice pinning, the RG flow of the disorder correlator $R(\phi)$ has been studied repeatedly in the past [39,43,45]. The RG flow is determined by equation (62) with $V_L(\phi) \equiv 0$. The fixed point functions $R^*(\phi)$ are always of the order ϵ, but their functional forms may be quite different depending on the bare functions $R_0(\phi)$ at $l = 0$. There exist mainly three different locally stable fixed points, each with its own basin of attraction. The corresponding solutions of equation (62) with $V_L(\phi) = 0$ will be analyzed in more detail for the different types of structure and disorder in the following subsections. Within this analysis the main focus is on the simplified scheme which allows for a reduction of the functional flow equation to a flow of at most two parameters. This novel representation will be helpful below for the inclusion of an additional crystal potential in the RG scheme.

5.1 Elastic manifolds

For the elastic manifold models, we have to distinguish between long-range correlated and short-range correlated random potentials. Both types of correlations can be physically realized for domain-walls ($N = 1$) in, for example, disordered ferroelectrics or Ising magnets. Whereas a random field leads to long-range correlated randomness, dilution forms short range correlated random bond disorder. In the following, we will generalize our considerations to structures with arbitrary N. For the rest of this section we set $V_L(\phi) = 0$ which corresponds to $W(\phi) = 0$ in equation (62).

5.1.1 Random fields

It is easy to show that the $R(\phi) \sim |\phi|$ behavior for large $|\phi|$ of the bare disorder correlator is preserved under the RG flow. Therefore we have to search for rotationally invariant solutions of the flow equation (62) with this asymptotic behavior. Power counting of this equation with respect to ϕ gives then the roughness exponent $\zeta^{RF} = (4 - D)/3$ independent of N. But we are interested also in the fixed point function $R^*(\phi)$ and the RG flow toward it. Using the ansatz $R(\phi) = \hat{R}(|\phi|)$, the flow

equation reduces after $\hat{R} \to R$ to

$$\frac{dR}{dl} = (\epsilon - 4\zeta)R(\phi) + \zeta\phi R'(\phi) + \frac{1}{2}[R''(\phi)]^2 - R''(0)R''(\phi)$$
$$+ (N - 1)\left\{\frac{1}{2}\frac{[R'(\phi)]^2}{\phi^2} - R''(0)\frac{R'(\phi)}{\phi}\right\}. \tag{64}$$

The fixed point solution $R^*(\phi)$ of this equation can be parameterized by its curvature $\Delta^* \equiv -R^{*''}(0)$, which is a measure for the disorder strength, and by its characteristic length scale ξ^*. With these parameters, the fixed point function can be written as

$$R^*(\phi) = \Delta^*\xi^{*2}r(\phi/\xi^*). \tag{65}$$

This relation defines the dimensionless function $r(u)$ with $u = \phi/\xi^*$ and $r''(0) = -1$. It describes the *functional form* of the fixed point solution and has a characteristic scale of order unity. Notice that there is a hole family of fixed points which are parameterized by different ξ^* since one has the freedom to choose an arbitrary overall length scale for ϕ in the Hamiltonian (1) without crystal potential $V_L(\phi)$. As we will see below, once a particular value for ξ^* has been chosen, the corresponding Δ^* is automatically fixed. From equations (64, 65) follows that the function $r(u)$ has to fulfill the equation

$$0 = \alpha r(u) + \beta u r'(u) + \frac{1}{2}[r''(u)]^2 + r''(u)$$
$$+ (N - 1)\left\{\frac{1}{2}\frac{[r'(u)]^2}{u^2} + \frac{r'(u)}{u}\right\} \tag{66}$$

where $\alpha = (\epsilon - 4\zeta)\xi^{*2}/\Delta^*$ and $\beta = \zeta\xi^{*2}/\Delta^*$ are numerical coefficients. From this one obtains the exponent

$$\zeta = \frac{\epsilon}{4 + \alpha/\beta}. \tag{67}$$

Generally, these coefficients are fixed first by the condition that $r(u)$ has the correct asymptotic behavior and second by the choice of an overall length scale for ϕ. From $r(u) \sim -|u|$ for large u follows the relation $\alpha = -\beta$. We choose a scale for ϕ such that $r(0) = -1$. That $r(0)$ has to be negative can be seen as follows. Evaluating equation (66) for small u, one easily obtains $\alpha = N/2r(0)$ due to $r''(0) = -1$. Since $\beta = \zeta\xi^{*2}/\Delta^* > 0$ we have $\alpha < 0$ and our choice of scale corresponds to $\alpha = -N/2$.

After we have determined the coefficients α and β, the fixed point function can be calculated in principle at least numerically by solving equation (66) for $r(u)$ with initial conditions $r(0) = -1$ and $r'(0) = 0$. But from a physical point of view, we are also interested in the evolution of the disorder under the RG transformation sufficiently close to the fixed point to study its stability or to calculate critical exponents of an unstable fixed point. In particular, this becomes important if we take into account a competing crystal potential which may lead to a new unstable fixed point associated with a roughening transition. Now, there is a *special* set of bare correlators $R_0(\phi)$ for which

the RG flow can be calculated on all length scales exactly. This special set is given by the two parameter family of functions $R_0(\phi) = \Delta_0\xi_0^2 r(\phi/\xi_0)$, *i.e.*, the functions are already of the functional fixed point form but differ by their bare strength Δ_0 and bare characteristic width ξ_0. The RG flow in the hyper-plane which is formed by these two parameters can be obtained by inserting the Ansatz

$$R(\phi) = \Delta(l)\xi^2(l)r(\phi/\xi(l)) \tag{68}$$

into the flow equation (64). Using the fact that $r(u)$ satisfies equation (66), this results in the following differential equation for $r(u)$,

$$A(l)r(u) + B(l)ur'(u) = 0, \tag{69}$$

where

$$A(l) = 2\xi\Delta\frac{d\xi}{dl} + \xi^2\frac{d\Delta}{dl} - (\epsilon - 4\zeta)\xi^2\Delta + \alpha\Delta^2, \tag{70}$$

$$B(l) = -\xi\Delta\frac{d\xi}{dl} - \zeta\xi^2\Delta + \beta\Delta^2. \tag{71}$$

In the last formulas we have dropped the l dependence of ξ and Δ. All the solutions $r(u)$ of equation (69) are simple powers of u and vanish for $u = 0$. But this is in contradiction to the correct form of $r(u)$ determined by equation (66), which is not a simple power of u and moreover finite for $u = 0$. Therefore such power law solutions cannot occur, and equation (69) is fulfilled if and only if $A(l) = B(l) = 0$ for all l. This condition straightforwardly leads to the RG flow equations

$$\frac{d\Delta}{dl} = (\epsilon - 2\zeta)\Delta - \frac{\alpha + 2\beta}{\xi^2}\Delta^2, \tag{72}$$

$$\frac{d\xi}{dl} = \left(-\zeta + \beta\frac{\Delta}{\xi^2}\right)\xi. \tag{73}$$

Flow equations of the same form but with different coefficients have been derived by Nattermann and Leschhorn [46] for random bond disorder, using the approximation that the bare Gaussian shape of $R(\phi)$ is preserved under the RG flow.

Before we come to the fixed point analysis of these equations, we will comment on the advantage of the two parameter representation over the functional flow of equation (64). For the Hamiltonian (1), without any perturbation from the crystal lattice, it has been shown that there exists a family of random field fixed points which is at least locally stable and represents the rough phase of the interface [43,45]. Since this family of fixed points lies in the hyper-plane of the two parameter flow, the RG flow starting from an arbitrary bare random field disorder correlator $R_0(\phi)$ should be described on sufficiently large length scales also by equations (72, 73).

Let us now turn back to the fixed point analysis of equations (72, 73). As explained above, we expect a line of stable fixed points resulting from the choice of the overall length scale for ϕ. This line is given by

$$\Delta^* = \frac{\epsilon - 2\zeta}{\alpha + 2\beta}\xi^{*2}, \tag{74}$$
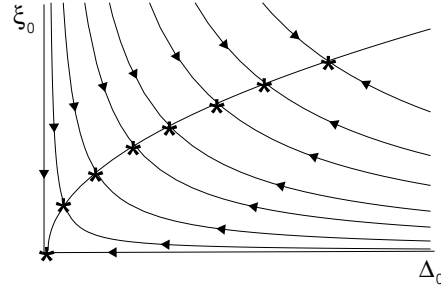
Fig. 5. Schematic RG flow to a line of fixed points in the hyper-plane formed by Δ_0 and ξ_0.

where

$$\xi^* = \xi_0\left(\frac{\alpha + 4\beta}{\epsilon}\frac{\Delta_0}{\xi_0^2}\right)^{\zeta/\epsilon} \tag{75}$$

depends on the bare parameters ξ_0 and Δ_0. The corresponding RG flow is shown in Figure 5. Linearizing about the fixed points, one finds the universal eigenvalues $\lambda_1 = 0$ and $\lambda_2 = -\epsilon$ corresponding to a redundant marginal and a stable direction, respectively. The leading irrelevant eigenvalue of the full functional RG flow for random field disorder is indeed given by λ_2 [45]. But notice that in general one cannot expect to obtain by the two parameter approach the *leading* irrelevant eigenvalue out of the infinite number of irrelevant eigenvalues.

The transversal displacement correlation function

$$C(\mathbf{x}) \equiv \frac{1}{N}\overline{\langle[\phi(\mathbf{x}) - \phi(\mathbf{0})]^2\rangle} \tag{76}$$

can be calculated perturbatively from the renormalized but non-rescaled effective parameter $\tilde{\Delta}(l) = \Delta(l)e^{(2\zeta-\epsilon)l}$ using $l = \ln(\Lambda/q)$. On length scales larger than the Larkin length, $|\mathbf{x}| \gg L_\Delta = [\epsilon N/(\alpha + 4\beta)\hat{\xi}_0^2/\Delta_0]^{1/\epsilon}$, we obtain

$$C(\mathbf{x}) = (N/\beta)\hat{\xi}_0^2(|\mathbf{x}|/L_\Delta)^{2\zeta}, \tag{77}$$

where we have explicitly considered the N-dependence of ξ_0 by writing $\xi_0^2 = N\hat{\xi}_0^2$. Notice that the Larkin length L_Δ and the coefficient of $C(\mathbf{x})$ remain finite for $N \to \infty$ due to $\alpha = -\beta = -N/2$.

For $D = 4$, the roughness exponent ζ vanishes and logarithmic scaling of the transversal displacement is expected. From the RG flow of the effective parameter $\tilde{\Delta}$ for $\epsilon = 0$, we find that the roughness grows only *sublogarithmically*,

$$C(\mathbf{x}) \sim \ln^\sigma(|\mathbf{x}|/a_0), \quad \sigma = \frac{2\beta}{\alpha + 4\beta}. \tag{78}$$

For random field disorder, we have the exponent $\sigma = 2/3$ independent of N.

5.1.2 Random bonds

As for random field disorder, it is straightforward to see that the functional behavior of the exponentially decaying

Table 2. Numerical values for β and the exponent ζ.

N	β	$\zeta/\epsilon = (4 + \alpha/\beta)^{-1}$
1	0.6244	0.2083
2	0.6010	0.1766
3	0.5807	0.1519
4	0.5635	0.1325
5	0.5491	0.1169

correlator $R_0(\boldsymbol{\phi})$ for random bond disorder is preserved by the RG flow [43]. To obtain a valid fixed-point function for short-range correlated disorder, therefore, we have to search for solutions of equation (64) with an exponential tail at large ϕ. The fixed-point function can still be written in the form of equation (65), and it remains the problem to determine the coefficients α and β such that equation (66) has an exponentially decaying solution $r(u)$ for the initial conditions $r(0) = 1, r'(0) = 0$. As in the random field case we have $\alpha = N/2r(0) = N/2$ by our choice of scale. Unfortunately, the conditions for the behavior of $r(u)$ do not fix the coefficient β uniquely since there exists a discrete family of solutions of equation (66) which decay exponentially at infinity. But it can be shown that only the function of the whole set of solutions corresponding to the largest value of β is stable with respect to short-range perturbations [43]. The corresponding value for β has to be calculated numerically. Solving equation (66) numerically, the unstable solutions can be distinguished from the stable one since they show oscillations instead of a simple exponential decay. The resulting values of β are shown in Table 2 together with the corresponding roughness exponents ζ for different N. The values for β decrease with N and approach $1/2$ for $N \to \infty$ corresponding to $\zeta/\epsilon \to 1/(4 + N)$.

With these values for the coefficients α and β the flow equations (72, 73) remain valid also for the random bond case. The RG flow is still given by equation (74) but with the exponent ζ from Table 2, and looks similar to that shown in Figure 5. For $N < \infty$, the correlation function $C(\mathbf{x})$ is given by equation (77) but with the values for ζ from Table 2. In contrast, for $N = \infty$ the roughness exponent vanishes and the manifold is only logarithmically rough,

$$C(\mathbf{x}) = 4\epsilon \hat{\xi}_0^2 \ln(|\mathbf{x}|/L_\Delta). \tag{79}$$

The exponent σ describing the sub-logarithmic scaling of equation (78) valid for $D = 4$ becomes $\sigma = 0.4166$ for $N = 1$ and approaches $\sigma = 2/(N + 4)$ for $N \to \infty$.

5.2 Periodic elastic media

The periodicity of the unrenormalized $R_0(\boldsymbol{\phi})$ has to be preserved under the RG flow, hence we have to search for fixed point solutions of equation (62) with an appropriate symmetry given by the reciprocal lattice vectors $\mathbf{Q}$. In general, one has to treat different lattice symmetries separately. For the simplest case, a square lattice, the fixed

point solution is separable,

$$R^*(\boldsymbol{\phi}) = \sum_{n=1}^{N} \hat{R}^*(\phi^n), \tag{80}$$

where $\hat{R}^*(\phi)$ is a periodic fixed point function of equation (62) with $N = 1$ and the ϕ^n are the components of $\boldsymbol{\phi}$. For a triangular lattice the situation is more difficult and we did not try to find a solution for this case. The $N = 1$ fixed point solution $\hat{R}(\phi)$ corresponds to the charge density wave case and has been calculated in reference [39]. The RG flow towards this fixed point can be analyzed by keeping track of the flow of the Fourier coefficients of $\hat{R}(\phi)$. For simplicity, we choose the periodicity as 2π and take $\hat{R}(\phi) \to R(\phi)$. Inserting the Fourier expansion

$$R(\phi) = \sum_{m=1}^{\infty} R_m \cos(m\phi) \tag{81}$$

into the functional flow equation (62) where we have to choose $\zeta = 0$ due to the periodicity, we obtain the following infinitely many flow equations for the coefficients R_m which are coupled to each other,

$$\begin{aligned}
\frac{dR_m}{dl} &= \epsilon R_m + \frac{1}{4} \sum_{m'=1}^{m-1} m'^2 (m - m')^2 R_{m'} R_{m-m'} \\
&\quad + \frac{1}{2} \sum_{m'=m+1}^{\infty} m'^2 (m' - m)^2 R_{m'} R_{m'-m} \\
&\quad - m^2 R_m \sum_{m'=1}^{\infty} m'^2 R_{m'}.
\end{aligned} \tag{82}$$

By performing simply the sums, it can be checked that a fixed point of this set of equations is given by $R_m^* = 2\epsilon/3m^4$. The corresponding series (81) can be summed up and yields the solution known from reference [39]. The flow towards this fixed point as well as its stability can be analyzed by rewriting the Fourier coefficients as

$$R_m = \frac{6}{\pi^2} \frac{\Delta}{m^4} + r_m \tag{83}$$

where $\Delta = -R''(0)$ with the fixed point value $\Delta^* = \epsilon \pi^2/9$. Substituting this Ansatz into equation (82), we see that the r_m flow to zero with eigenvalues $\lambda_m = \epsilon(2/3 - m - 2m^2/3)$ whereas the flow of Δ is determined by

$$\frac{d\Delta}{dl} = \epsilon \Delta - \frac{9}{\pi^2} \Delta^2. \tag{84}$$

Since we are interested in the RG flow on sufficiently large length scales, we will therefore assume here the particularly simple functional form of the fixed point by dropping the r_m. This approximation is justified on length scales larger than the Fukuyama-Lee length $L_\Delta = \Delta^{-1/\epsilon}$ where the parameters r_m approach zero. The RG flow towards the fixed point is then described by the single parameter flow of equation (84).

The transversal displacement correlation function growths only logarithmically on scales beyond the Fukuyama-Lee length L_Δ,

$$C(\mathbf{x}) = 2\frac{\pi^2}{9}\epsilon \ln(|\mathbf{x}|/L_\Delta) \qquad (85)$$

with a universal coefficient which may depend on the actual lattice symmetry. The coefficient given here applies to a square lattice with a periodicity of 2π.

6 The roughening transition

To study the effect of a finite lattice pinning potential $V_L(\phi)$ upon the large scale behavior of elastic objects, we have to analyze the full set of functional RG equations (61–63). As has been shown is Section 5, while the same functional RG equations apply for the different types of elastic objects and bare disorder correlations, the corresponding solutions are quite different. Therefore, we will discuss the analysis of the RG flow in the following subsections separately for elastic manifolds and elastic periodic media.

6.1 Elastic manifolds

For the case of elastic manifolds, the functional RG flow of the disorder correlator $R(\phi)$ has been reduced already to a flow of two parameters for vanishing lattice pinning in Section 5. To develop the RG analysis for finite $V_L(\phi)$, it is important to note that the functional form of the flow equation for $R(\phi)$ is not changed. Indeed, a finite lattice potential leads only to a shift of $\epsilon = 4 - D$ by the constant $2\mathcal{P}_0[W(\phi)]$, as can be seen easily from equation (62). Therefore, the RG flow of $R(\phi)$ can be replaced again by the two-parameter flow of equations (72, 73) but with a shifted ϵ. For the lattice potential we have to consider only the first harmonics, and we assume in the following the simple form of equation (2) with

$$V(\phi) = v \cos\left(\frac{2\pi}{a}\phi\right) \qquad (86)$$

for all components of the vector ϕ.

To begin with, we calculate the projection of the function $W(\phi)$ defined in equation (60) onto the lowest harmonic $E_0(\phi) = 1$. Using equation (86) and $\partial_i\partial_j R(\mathbf{0}) = -\Delta\delta_{ij}$, the function $W(\phi)$ becomes

$$W(\phi) = -\Delta v^2 \frac{(2\pi)^6}{a^6} \sum_{i=1}^{N} \sin^2\left(\frac{2\pi}{a}\phi^i\right). \qquad (87)$$

After projection onto the lowest harmonic, this equation reduces to

$$\mathcal{P}_0[W(\phi)] = -\frac{1}{2}\Delta v^2 \frac{(2\pi)^6}{a^6} \qquad (88)$$

since $\sin^2(y) = (1 - \cos(2y))/2$. Note that the negative eigenvalue θ of the temperature flow, see equation (61), is also shifted by this constant to a larger value. Physically, this corresponds to an increased elastic stiffness of the manifold due to the lattice potential.

The RG flow of the first harmonic of the lattice potential can be obtained by inserting the sum of the first harmonics (86) for $V_L(\phi)$ in equation (63) and projecting again the whole equation onto the first harmonics. To treat the second term $\sim \phi^i$ in equation (63) properly, one has to rescale also the periodicity a which leads to the trivial flow $da/dl = -\zeta a$. After the projection, the term which is quadratic in V_L vanishes since it contributes only to the second harmonics. Both the term cubic in V_L and the term $\mathcal{P}_0[W]V_L$ from the stiffness renormalization are of order v^3. Using for the projection of W the relation $\cos^3(y) = (3\cos(y) + \cos(3y))/4$, we obtain the following parameter RG flow,

$$\frac{dT}{dl} = \left[2 - D - 2\zeta - \frac{1}{2}\Delta v^2 \frac{(2\pi)^6}{a^6}\right]T, \qquad (89)$$

$$\frac{d\Delta}{dl} = (\epsilon - 2\zeta)\Delta - \left[\frac{\alpha + 2\beta}{\xi^2} + \frac{(2\pi)^6}{a^6}v^2\right]\Delta^2, \qquad (90)$$

$$\frac{d\xi}{dl} = \left[-\zeta + \beta\frac{\Delta}{\xi^2}\right]\xi, \qquad (91)$$

$$\frac{dv}{dl} = \left[2 - 2\zeta - \frac{1}{2}\frac{(2\pi)^2}{a^2}\Delta\right]v - \frac{7}{8}\frac{(2\pi)^6}{a^6}\Delta v^3, \qquad (92)$$

$$\frac{da}{dl} = -\zeta a. \qquad (93)$$

It is important to note that these flow equations are symmetric with respect to $v \to -v$ as could be expected for a periodic potential since this transformation corresponds only to a shift in ϕ^i by $a/2$. Naively, one expects for the coefficients α and β the same relations as given below equation (66) but with shifted ϵ. But these relations have to be reexamined later since it turns out that ξ^{*2}/Δ^* diverges at the new fixed point describing the roughening transition.
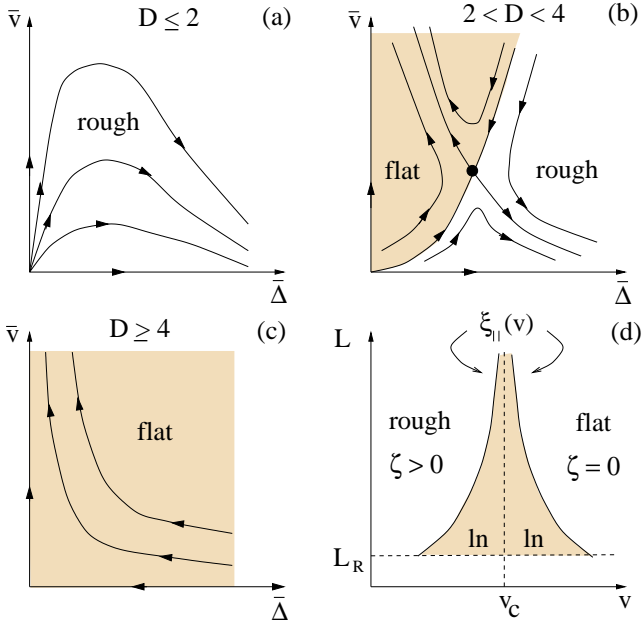
To analyze the above scaling transformations, it is useful to introduce the new variables $\bar{\Delta} \equiv (2\pi/a)^2\Delta$, $\bar{\xi} \equiv (2\pi/a)\xi$ and $\bar{v} \equiv (2\pi/a)^2 v$. By this change of variables, the roughness exponent ζ is eliminated from the coupled flow equations. To finally obtain ζ, we have to evaluate the relations for α or β in terms of the flow of the new variables along the critical line flowing into the fixed point. In terms of the new variables, we have

$$\frac{dT}{dl} = \left[2 - D - 2\zeta - \frac{1}{2}\bar{\Delta}\bar{v}^2\right]T, \qquad (94)$$

$$\frac{d\bar{\Delta}}{dl} = \epsilon\bar{\Delta} - \left[\frac{\alpha + 2\beta}{\bar{\xi}^2} + \bar{v}^2\right]\bar{\Delta}^2, \qquad (95)$$

$$\frac{d\bar{\xi}^2}{dl} = 2\beta\bar{\Delta}, \qquad (96)$$

$$\frac{d\bar{v}}{dl} = \left[2 - \frac{1}{2}\bar{\Delta}\right]\bar{v} - \frac{7}{8}\bar{\Delta}\bar{v}^3. \qquad (97)$$

Fig. 6. Schematic RG flow for $N < \infty$ as a function of the disorder variable $\bar{\Delta}$ and the lattice strength $\bar{v}$ for (a) $D \leq 2$, (b) $2 < D < 4$ and (c) $D \geq 4$. Note that the fixed point associated with the rough phase is shifted here to $\bar{\Delta} = \infty$. (d) shows the length scale L dependent roughness near the roughening transition where the correlation length $\xi_\parallel(v)$ diverges.

Before we study the case $v \neq 0$, it should be mentioned that the stable fixed point of the rough phase is located at $\bar{v} = 0$, $\bar{\Delta} = \infty$ in terms of the new variables since the periodicity a flows exponentially fast to zero. Now we turn to the fixed point analysis for finite $\bar{v}$ and $N < \infty$. The case $N = \infty$ will be discussed separately in Section 6.4. To obtain a fixed point with a finite value for $\bar{v}$ from equation (97), the parameter $\bar{\Delta}$ has to flow along a critical line to a finite value $\bar{\Delta}^*$. The corresponding fixed point value for $\bar{v}$ is then given by $\bar{v}^{*2} = 4(4/\bar{\Delta}^* - 1)/7$. As a consequence of equation (96) and since $\beta > 0$, one obtains the asymptotic behavior $\bar{\xi}^2 = 2\beta\bar{\Delta}^*l$ up to sub-linear corrections. But this divergence of $\bar{\xi}^2$ means that we can drop the first term in the brackets of equation (95) for the fixed point analysis. This leads to the fixed point values, valid to lowest order in ϵ,

$$\bar{\Delta}^* = 4 - \frac{7}{4}\epsilon, \quad \bar{v}^{*2} = \frac{\epsilon}{4} \cdot \tag{98}$$

As one may expect, $\bar{v}^*$ vanishes when the upper critical dimension is approached, justifying the ϵ-expansion. It should be noted that $\bar{v}^*$ has the meaning of a (rescaled) mass for the field ϕ. The second small parameter in the double expansion with respect to both pinning potentials is Δ, which is indeed small at the new fixed point since $\Delta \sim 1/l$ along the critical line as we will see below. Moreover, it should be mentioned that the fixed point value $\bar{\Delta}^*$ vanishes for $\epsilon = 16/7$ corresponding to a shift of this fixed point to the $\bar{v}$ axis for $D = 12/7$, see Figure 6. Note that this is, despite the lowest order ϵ result, in approximate

agreement with the absence of a roughening transition for $D \leq 2$ as predicted by scaling arguments in Section 3.

Linearizing around this fixed point, we obtain, in lowest order in ϵ, the universal eigenvalues $\lambda_\pm = \pm 2\sqrt{\epsilon}$. Since the fixed point has an unstable direction, it has to be associated with the roughening transition. In the flat phase, the size of typical excursions of the manifold from the preferred minimum of the lattice potential defines the longitudinal correlation length

$$\xi_\parallel \sim |v - v_{0,c}|^{-\nu_\parallel}, \quad \nu_\parallel = \frac{1}{2\sqrt{\epsilon}} \cdot \tag{99}$$

Interestingly, $\nu_\parallel$ does not dependent on α, β and is therefore universal for random field and random bond disorder. The same expression for $\nu_\parallel$ has been obtained previously for the *thermal* roughening transition but with $\epsilon = 2 - D$ [21].

To determine the critical roughness exponent ζ_c at the roughening transition, we have to re-examine the relations between the coefficients α and β and the fixed point values. Paying attention to the fact that Δ approaches zero at the new fixed point, we obtain the refined expression

$$\alpha = \lim_{l\to\infty} \frac{\bar{\xi}^2}{\bar{\Delta}} \left[\epsilon - 2\zeta - \bar{\Delta}\bar{v}^2 - \frac{1}{\bar{\Delta}}\frac{d\bar{\Delta}}{dl} \right], \tag{100}$$

which turns out to be equivalent to

$$\beta = \lim_{l\to\infty} \zeta \frac{\bar{\xi}^2}{\bar{\Delta}} \cdot \tag{101}$$

From the last expression we see that ζ has to flow along the critical line asymptotically according to

$$\zeta = \frac{1}{2l} \tag{102}$$

since $\bar{\xi}^2/\bar{\Delta} = 2\beta l$. Therefore, at the transition we have $\zeta_c = 0$ and the roughness of the manifold grows only *logarithmically*. Due to $\zeta = 1/2l$ for large l, the periodicity of the lattice potential flows only algebraically to zero, $a \sim l^{-1/2}$, in agreement with the logarithmic scaling at the transition. Therefore, the renormalized width $\xi \sim \bar{\xi}/a$ of the disorder correlator flows to a finite value ξ^* at the new fixed point. Notice that at this fixed point one has no longer the freedom to choose an arbitrary overall length scale for ϕ due to the fixed periodicity a_0 of the lattice potential. As a consequence, there is no line of fixed points connected by a redundant operator as in the case of vanishing lattice potential.

The free energy fluctuations grow with length as L^θ, where θ is defined by equation (61). In the rough phase the tilt symmetry of the Hamiltonian (1) guarantees that the temperature is renormalized only by scale changes. This leads to the exact result $\theta = D - 2 + 2\zeta$. The relevance of the lattice potential results in an additional renormalization of temperature and therefore a different exponent θ_c at the transition. Independent of α and β, we obtain from the fixed point values of equation (98) to lowest order in ϵ the result

$$\theta_c = 2 - \frac{\epsilon}{2} \cdot \tag{103}$$

The cross-over length scale L_R introduced in Section 3 can also be obtained from the RG flow of $\bar{\Delta}$. This length corresponds to the scale where the roughness of the manifold changes from algebraic to logarithmic growth on both sides of the transition. In terms of the RG flow, $L_R = a_0 e^{l_R}$ is determined by the scale l_R where $\bar{\Delta}(l)$ approaches its asymptotic fixed point value $\bar{\Delta}^*$. To estimate l_R, one can integrate equation (95) with $\bar{v} = 0$ to obtain a primary solution. The effect of the $\bar{v}^2$-term can subsequently be included by matching the primary solution $\bar{\Delta}(l)$ and $\bar{\Delta}^*$ at l_R. Doing so, we get

$$
L_R = L_\Delta \left(\frac{\alpha + 4\beta}{N} \frac{\bar{\Delta}^*}{\epsilon} \frac{a_0^2}{\hat{\xi}_0^2} \right)^{1/2\zeta}, \qquad (104)
$$

where ζ is the roughness exponent of the algebraic regime at smaller scales. It is given by the exponent ζ of the rough phase for $\hat{\xi}_0 \ll a_0$ and $\zeta = \epsilon/2$ for $\hat{\xi}_0 \gg a_0$. This is in agreement with the scaling result of equation (15) if v_0 is replaced there by $v_{0,c}$ of equation (17).

Beyond the length L_R and sufficiently close to the transition where $\xi_\parallel > |\mathbf{x}|$, the asymptotic behavior of the transverse difference correlation function is given by

$$
C(\mathbf{x}) = \frac{1}{N} \overline{\langle [\phi(\mathbf{x}) - \phi(\mathbf{0})]^2 \rangle} \sim \ln(|\mathbf{x}|/L_R) \qquad (105)
$$

on both sides of the RT, see Figure 6d. Beyond $\xi_\parallel$ the roughness crosses over to the power law $C(\mathbf{x}) \sim (|\mathbf{x}|/\xi_\parallel)^{2\zeta}$ in the rough phase. On the flat side of the transition $C(\mathbf{x})$ saturates on scales larger than $\xi_\parallel$ at a finite value $\sim \ln(\xi_\parallel/L_R)$.

The phase boundary between the rough and the flat phase can be obtained from the condition that the primary solution of equation (97), neglecting the $\bar{v}^3$ term, and the fixed point value $\bar{v}^*$ match at the cross-over length l_R. This condition leads to the result

$$
v_{0,c}(\Delta_0, \hat{\xi}_0) = g(\epsilon) a_0^2 \left(\frac{\hat{\xi}_0}{a_0} \right)^{2/\zeta} \left(\frac{\Delta_0}{\hat{\xi}_0^2} \right)^{2/\epsilon}, \qquad (106)
$$

which is in agreement with the estimate of equation (24) derived from scaling arguments for random field disorder. The coefficient $g(\epsilon)$ is given to lowest order in ϵ by

$$
g(\epsilon) = \frac{\epsilon}{2} \left(\frac{\epsilon N}{\alpha + 4\beta} \right)^{1/\zeta - 2/\epsilon} (4e)^{-1/\zeta}. \qquad (107)
$$

In both expressions above, ζ is always the exponent of the rough phase for $\hat{\xi}_0 \ll a_0$ and $\zeta = \epsilon/2$ for $\hat{\xi}_0 \gg a_0$. As can be seen easily from the behavior of $g(\epsilon)$, the threshold $v_{0,c}$ vanishes exponentially fast for $\epsilon \to 0$. This is in agreement with the fact that in four dimensions an arbitrarily small lattice potential leads to a flat phase due to the sub-logarithmic roughness for $v \equiv 0$, *cf.* equation (78). The schematic RG flow for $2 < D < 4$ is shown together with that expected from the scaling arguments of Section 3 for $D \leq 2$ in Figure 6.

6.2 Interfaces in dipolar systems

As shown in Section 3, in the physically interesting case $D = 2$ the manifold is rough beyond the cross-over length L_R even for a finite crystal potential. Although L_R is exponentially large for weak disorder, there exists, strictly speaking, no roughening transition for $D = 2$. However, the transition is expected to be seen even for $D = 2$ in systems with dipolar interactions as already noted in reference [35]. In these systems ferroelectric or magnetic domain walls ($N = 1$) separate regions of opposite polarization or magnetization. Assuming that the dipoles interact *via* a three-dimensional Coulomb force and that the dipolar axis ρ is parallel to the wall, one obtains for $D > 1$ in harmonic approximation the modified elastic energy [47,48]

$$
E_{\rm el} = \frac{\gamma}{2} \int \frac{d^D \mathbf{q}}{(2\pi)^D} q^2 \left(1 + g \frac{q_\rho^2}{q^{D+1}} \right) \phi_{-\mathbf{q}} \phi_{\mathbf{q}}, \qquad (108)
$$

where g measures the relative strength of the dipolar interaction. As can be easily seen from equation (108), the dipolar interaction increases the elastic stiffness of the interface on large scales. As a result, the upper critical dimension D_c should decrease compared to the case of a short-ranged elastic kernel $\sim q^2$ with $D_c = 4$.

There are mainly two differences compared to the usual case discussed before. First, the large scale behavior of the interface is described correctly if we take the stiffness constant to be an effective $\mathbf{q}$-dependent function $\tilde{\gamma}(\mathbf{q}) \sim \sqrt{g} \gamma |\mathbf{q}|^{(1-D)/2}$. This can be seen by writing $q_\rho = q \cos(\varphi)$ and performing the angular integration over φ in the Fourier representation of the free two-point function. This integration yields an additional factor $\sim |\mathbf{q}|^{(D-1)/2}$ in the limit $|\mathbf{q}| \to 0$ which can be absorbed in $\tilde{\gamma}$. Repeating the RG analysis with this modified $\tilde{\gamma}$, the form of the terms in the flow equations arising from scale changes remains unchanged if we replace $\epsilon = 4 - D$ by

$$
\epsilon = \frac{3}{2}(3 - D). \qquad (109)
$$

Therefore, the upper and lower critical dimension is shifted to $D_c = 3$ and $D_l = 5/3$, respectively, and there exists a roughening transition for two-dimensional dipolar interfaces. The second difference arises from the fact that the long-ranged part of the elastic kernel is not renormalized, in contrast to the situation for local elasticity. As a consequence, the novel fixed point describing the roughening transition no longer exists and the transition may become of first order.

6.3 Periodic elastic media

Having established the existence of a roughening transition for single elastic manifolds, we now turn to the case of periodic elastic media. From the analysis of Section 5.2 we

know that the correlation function $C(\mathbf{x})$ behaves logarithmically for $|\mathbf{x}| > L_\Delta$ in the rough unlocked phase (U) described by the stable $T = 0$ fixed point U^*. Therefore, one can expect a logarithmic scaling of ϕ also at the roughening transition, hence we set in this section $\zeta = 0$ from the very beginning. To extend the RG analysis to $V_L(\phi) \neq 0$, we follow the treatment presented above for elastic manifolds. In the following, we will focus on the particular case of a square lattice for the elastic medium. Then we are able to make use of the reduction of the $R(\phi)$-flow to the single parameter flow for Δ derived in Section 5.2, *cf.* equation (84). Again, a finite lattice potential changes this equation only by a shift in ϵ. For simplicity, we set the periodicity of the elastic medium to $l = 2\pi$ in the following such that $p = 2\pi/a_0$ on all length scales since transversal lengths are not rescaled here. Then the scaling equations for elastic media read

$$\frac{dT}{dl} = (2 - D - \frac{1}{2}p^6 \Delta v^2)T, \tag{110}$$

$$\frac{d\Delta}{dl} = \epsilon\Delta - \frac{9}{\pi^2}\Delta^2 - p^6 v^2 \Delta^2, \tag{111}$$

$$\frac{dv}{dl} = \left(2 - \frac{p^2}{2}\Delta\right)v - \frac{7}{8}p^6 \Delta v^3. \tag{112}$$

From the scaling arguments presented in Section 3, one may expect that for $p < p_c = 6/\pi\sqrt{\epsilon}$ weak disorder is always irrelevant due to the logarithmic roughness in the phase U. For $p > p_c$ a weak periodic potential is irrelevant, but one expects that it becomes a relevant perturbation once v_0 exceeds a critical value $v_{0,c}$. Therefore, $v_{0,c}$ has to vanish if $p \to p_c^+$, and a new unstable fixed point corresponding to a roughening transition should be accessible perturbatively in $\epsilon = 4 - d$ and the second small parameter $\mu = p^2/p_c^2 - 1$.

Indeed, there exists a new unstable $T = 0$ fixed point F^* which approaches the stable fixed point describing the rough phase if $\mu \to 0$. It is parameterized to lowest order in ϵ and μ by

$$\Delta^* = \frac{\pi^2}{9}\epsilon(1 - \mu), \quad p^2 v^* = \frac{\sqrt{\epsilon\mu}}{2}. \tag{113}$$

Linearization around this fixed point gives the eigenvalues $\lambda_1 = -\epsilon$ and $\lambda_2 = 4\mu$. Thus, one has to identify this unstable fixed point with the roughening transition. The longitudinal correlation length $\xi_\|$ beyond which the periodic medium is locked into the minima of the lattice potential diverges according to

$$\xi_\| \sim |v - v_{0,c}|^{-\nu_\|}, \quad \nu_\| = \frac{1}{4\mu} \tag{114}$$

if the transition is approached from the flat side. On the rough side of the transition $\xi_\|$ is infinite, in contrast to the situation for single elastic manifolds. The resulting phase diagram is characterized by a critical line $\Delta_c(v)$ separating the flat or commensurate (C) and rough, unlocked phase (U), see Figure 7. The position of this critical line is given by the scaling result $v_{0,c} \approx p^{-2}\Delta_0^{2/\epsilon}$ derived in Section 3.
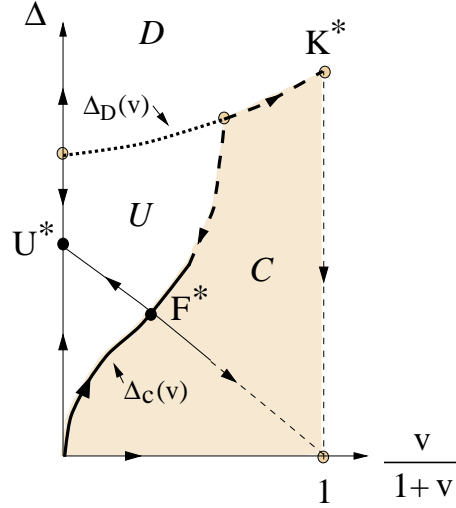
Fig. 7. Schematic RG flow for $p > p_c$ in the v-Δ-plane. A critical line $\Delta_c(v)$ with fixed point F^* separates the flat (C) and rough, unlocked (U) phase. For $p < p_c$ the fixed points F^* and U^* merge. Since for large disorder strength Δ topological defects will proliferate, we expect a disordered phase D above the line $\Delta_D(v)$ as will be explained in Section 8. While the RG flow in this range is not yet clear, the transition from the C to the D phase is probably in the universality class of the random field p-state clock model.

To characterize the order of the periodic medium, we introduce the translational order parameter

$$\Psi(\mathbf{x}) = \rho_1 \exp(i\phi(\mathbf{x})). \tag{115}$$

For simplicity, we study here the case of a scalar field ($N = 1$) only. Inside the C phase, one has a nonzero expectation value $\overline{\langle\Psi(\mathbf{x})\rangle}$. The correlation function of the fluctuations $\delta\Psi(\mathbf{x}) = \Psi(\mathbf{x}) - \overline{\langle\Psi(\mathbf{x})\rangle}$ decays exponentially in this phase,

$$K(\mathbf{x}) = \overline{\langle\delta\Psi(\mathbf{x})\delta\Psi^*(\mathbf{0})\rangle} \sim \exp(-|\mathbf{x}|/\xi_\|). \tag{116}$$

Approaching the transition from the C phase, the order parameter vanishes continuously as

$$\overline{\langle\Psi(\mathbf{x})\rangle} \sim (v_0 - v_{0,c})^\beta, \quad \beta = \frac{\pi^2}{18}\epsilon\nu_\|. \tag{117}$$

In contrast, at the transition and in the rough phase, $v_0 \leq v_{0,c}$, the periodic medium is unlocked with $\overline{\langle\Psi(\mathbf{x})\rangle} = 0$ and the correlation function shows a power law decay,

$$K(\mathbf{x}) \sim |\mathbf{x}|^{4-D-\bar\eta}, \quad \bar\eta = (1 + \pi^2/9)\epsilon. \tag{118}$$

At the transition the 'violation of hyperscaling' exponent is increased from the exact value $\theta = D - 2$ in the rough phase to

$$\theta_c = D - 2 + \epsilon\mu/2 \tag{119}$$

due to the renormalization of the elastic stiffness of the medium. The critical exponents mentioned above fulfill all scaling relations and exponent inequalities which hold for random field models with a discrete symmetry of the order parameter [49,50].

6.4 The limit N = ∞

It is important to note that the order as well as the critical exponents $\nu_\parallel$ and ζ_c of the roughening transition do not depend on N as long as N is finite. For arbitrary N, the roughening transition of manifolds in random bond systems has also been studied within a variational approach by Bouchaud and Georges (BG) [35]. At $T = 0$ and for $\hat{\xi}_0 \ll a_0$ these authors find a first order transition between a glassy rough and a glassy flat phase. In the glassy rough phase they obtain the Flory result $\zeta = \epsilon/5$ which is known to be not correct for small ϵ. We attribute this as well as the first order nature of the transition to the use of the variational method which is known to give spurious first order transitions [51]. However, the variational approach is expected to become exact for $N = \infty$. Since our results seem to be in contrast to the $N = \infty$ results of BG, we will study the RG flow for elastic manifolds in this limit now.

Our discussion starts again with the flow equations (95–97). To have a finite bare starting value for $\bar{\xi}$ in the limit $N \to \infty$, we rescale this parameter according to $\bar{\xi}^2 \to N\bar{\xi}^2$. For random field disorder, the structure of the flow equations remains unchanged in the limit $N \to \infty$ since $\beta = N/2$. Therefore, the transition is still of second order and the phase boundary is given by equation (106) with the N-independent coefficient of equation (107). In contrast, for random bond disorder the manifold is only logarithmically rough in the case $N = \infty$, cf. equation (79), and we expect a roughening transition similar to that of periodic media. Indeed, due to the above rescaling of $\bar{\xi}$ and $\beta = 1/2$ we obtain $d\bar{\xi}^2/dl = 0$ and, therefore, equation (95) reduces to

$$\frac{d\bar{\Delta}}{dl} = \epsilon\bar{\Delta} - \left[\frac{1}{2p^2} + \bar{v}^2\right]\bar{\Delta}^2, \qquad (120)$$

where $p = 2\pi\hat{\xi}_0/a_0$ is a constant. Comparing this equation with the flow equation (111) of Δ for periodic media, we conclude that for $p < p_c = \sqrt{2/\epsilon}$ the manifold is already in the flat phase for an infinitesimally small v_0. A roughening transition at a finite v_0 exists only for $p > p_c$, and then the correlation length diverges as described by equation (114).

The variational calculation of BG applies in the random bond case where $\hat{\xi}_0 \ll a_0$, i.e. for $p < p_c$. Therefore, for $N = \infty$ we expect no transition at a finite v_0. Indeed, this is in agreement with the result for the phase boundary of BG in the limit $N = \infty$. The resulting transition at $v_{0,c} = 0$ for $p < p_c$ is not described by a fixed point of our RG equations and we have been unable to ascertain definitely the nature of the transition in this case. We will discuss this in more detail in Section 8 in the context of periodic media.

6.5 Incommensurate phases

So far we have considered only periodic elastic media with a periodicity $l = pa_0$ which is exactly an integer multiple of the crystal lattice periodicity a_0. But in general, this condition is not fulfilled exactly in real systems and one has to assume a shifted lattice constant

$$l = pa_0(1 - pa_0\delta) \qquad (121)$$

for the elastic medium, where δ is a small misfit. For example, δ can be changed in flux line lattices by tuning the external magnetic field or in charge density waves by changing the temperature. It is well-known from the sine-Gordon model subject to thermal fluctuations that above some critical value δ_c of the misfit, the incommensurability is compensated by the formation of domain walls or solitons of intrinsic width given by the correlation length $\xi_\parallel$ [52]. Across these walls the phase field $\phi(\mathbf{x})$ changes by $2\pi/p$. In the following, we specialize our discussion of the incommensurate phases to the case of a scalar field ($N = 1$).

The effect of a finite misfit can be described by adding a linear gradient term to the Hamiltonian defined in equation (1), such that the elastic term is replaced by

$$\frac{\gamma}{2}\int d^D\mathbf{x}\left\{\boldsymbol{\nabla}\phi - \boldsymbol{\delta}\right\}^2 \qquad (122)$$

with $\boldsymbol{\delta} = \delta\hat{\mathbf{z}}$ and $\hat{\mathbf{z}}$ the modulation direction of the periodic medium. For completeness we note that for a vanishing lattice potential V_L the misfit δ can be eliminated by the transformation $\phi(\mathbf{x}) \to \phi(\mathbf{x}) + \delta z$ due to the statistical symmetry of the disorder under a shift in ϕ. The linear gradient term in equation (122) can be integrated out leading to the contribution

$$-\gamma\delta\int d^D\mathbf{x}\frac{2\pi}{p}\frac{1}{\ell} \qquad (123)$$

to the Hamiltonian (1), where we have introduced the mean soliton density $\ell^{-1} = p[\phi(z = L) - \phi(z = 0)]/2\pi L$ for a system of size L in $\hat{\mathbf{z}}$-direction.

To study the case of finite lattice pinning, a direct RG treatment of the Hamiltonian (1) with an additional term (123) is not justified since a finite soliton density ℓ^{-1} induces linearly growing contribution $\sim \ell^{-1}z$ to the field $\phi(\mathbf{x})$ which cannot be Fourier expanded. To avoid this problem, we go back to periodic boundary conditions by the transformation $\phi(\mathbf{x}) \to \phi(\mathbf{x}) - 2\pi z/p\ell$ [53]. Note that we treat the mean soliton distance ℓ as a fixed parameter which is not renormalized and has to be determined later by minimizing the free energy of the soliton lattice. In the commensurate phase (C) for $\delta < \delta_c$, the soliton density vanishes and hence the RG analysis for $\delta = 0$ applies. To estimate δ_c, we compare the energy gain of a soliton per unit area, $-\gamma\delta 2\pi/p$, with its cost for vanishing misfit, $\gamma\sqrt{v_{eff}}2\pi/p$, where $v_{eff} = (p\xi_\parallel)^{-2}$ denotes the effective strength of the lattice potential renormalized by disorder. This leads to the result

$$\delta_c \approx \frac{1}{p\xi_\parallel} = \sqrt{v_0}\left(1 - \frac{\Delta_0}{\Delta_{0,c}}\right)^{\nu_\parallel}, \qquad (124)$$

where we have used equation (114). The corresponding phase diagram for fixed v_0 is shown in Figure 8. Since for
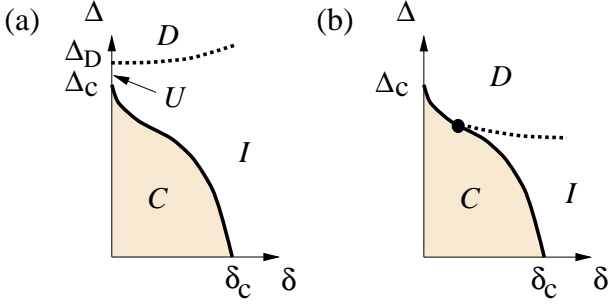
Fig. 8. Schematic phase diagrams for finite misfit δ at fixed crystal potential strength v_0 for $p > p_c$ (a) and $p < p_c$ (b). Due to the proliferation of topological defects a disordered phase is expected above a disorder strength Δ_D.

$p < p_c$ the lattice potential is always relevant for weak disorder, there exists in this case for large enough disorder a direct transition to a disordered phase (D). This transition is not described by our approach since it is driven by the proliferation of topological defects as will be explained in Section 8. In deriving expression (124), we have neglected a possible additional reduction of δ_c by fluctuations of the solitons on scales beyond $\xi_\parallel$ which have not been integrated out by the RG.

In the incommensurate phase (I) the above transformation to periodic boundary conditions induces a spatial oscillation in the amplitude of the lattice potential,

$$V_L(\phi) = v_0 \cos(p\phi - 2\pi z/\ell). \qquad (125)$$

Notice that the same oscillating pinning potential describes vicinal surfaces which are tilted by a small angle $\theta = 2\pi/p\ell$ with respect to the crystal planes [54]. In the RG calculations, this leads to an additional factor $\exp(i2\pi z/\ell)$ in the integral of equation (42). When the lattice potential is relevant, $\Delta_0 < \Delta_{0,c}$, there are two length scales: ℓ and the correlation length $\xi_\parallel$.

If $\xi_\parallel \ll \ell$, the RG up to $\xi_\parallel$ is insensitive to the oscillations along the z-direction and the soliton lattice can be described in terms of an effective free energy. The corresponding free energy density is given by [48]

$$f(\ell) \simeq \frac{1}{\ell}\left\{\sigma\left(1 - \frac{\delta}{\delta_c}\right) + 4\sigma e^{-\ell/\xi_\parallel} + B(D)\sigma\ell^{-1/\bar{\beta}}\right\}. \qquad (126)$$

Here the first term is the free energy of a soliton per unit area, the second term is the bare soliton repulsion, and the last part describes the steric repulsion caused by collisions of the solitons. The effective soliton tension is $\sigma = 8\gamma/p^2\xi_\parallel$, $B(D)$ is a coefficient which vanishes for $D > 5$ and $\bar{\beta} = \zeta/(2 - 2\zeta) = (5 - D)/2(D - 2)$ where $\zeta = (5 - D)/3$ is the roughness exponent of the soliton walls subject to random field disorder. Minimizing the free energy, we obtain the mean soliton distance near the IC-transition

$$\ell \sim (\delta - \delta_c)^{-\bar{\beta}}. \qquad (127)$$

To determine the translational order inside the I phase, the soliton lattice itself can be considered, on scales larger than ℓ as a periodic elastic medium with a disorder correlator $R_0(\phi)$ of periodicity ℓ. The corresponding Hamiltonian is given by equation (1) with $V_L = 0$ and $N = 1$ but with anisotropic elasticity. The elastic constants are $\gamma_\parallel = \sigma/\ell$ parallel to the solitons and $\gamma_\perp = \ell^2 f''(\ell)$ in $\hat{\mathbf{z}}$ direction. Rescaling the z coordinate according to $\sqrt{\gamma_\parallel/\gamma_\perp}z \to z$, we can achieve again an isotropic elastic term with $\gamma = \sqrt{\gamma_\parallel\gamma_\perp}$. Using the result of equation (85) we obtain a logarithmically diverging correlation function for the soliton displacement field $u(\mathbf{x})$,

$$\overline{\langle[u(\mathbf{x}) - u(\mathbf{0})]^2\rangle} = \frac{4 - D}{36}\ell^2 \ln\left(\frac{\mathbf{x}_\parallel^2}{L_\parallel^2} + \frac{z^2}{L_\perp^2}\right). \qquad (128)$$

Here the Larkin lengths $L_\parallel \sim (\ell^4\gamma_\parallel^{3/2}\gamma_\perp^{1/2})^{1/(4-D)}$ and $L_\perp = \sqrt{\gamma_\perp/\gamma_\parallel}L_\parallel$ are the correlations length beyond which the logarithmic divergence becomes asymptotically exact. Since $\gamma_\parallel \sim \ell^{-1}$ and $\gamma_\perp \sim \ell^{(\zeta-2)/\zeta} = \ell^{-(D+1)/(5-D)}$ for random fields, both correlation lengths diverge if the IC-transition is approached from the I phase as

$$L_\parallel \sim \ell^{3/(5-D)} \sim (\delta - \delta_c)^{-3/2(D-2)} \qquad (129)$$

$$L_\perp \sim \ell \sim (\delta - \delta_c)^{-(5-D)/2(D-2)} \qquad (130)$$

similar to the situation for the IC-transition in the presence of thermal fluctuations only [48,55].

The behavior of the correlation function $K(\mathbf{x})$ of the fluctuations of the translational order parameter $\Psi(\mathbf{x})$ can be easily obtained from equation (128). The soliton lattice shows quasi long range order with

$$K(\mathbf{x}) = \rho_1^2 \cos\frac{2\pi z}{p\ell}\left(\frac{\mathbf{x}_\parallel^2}{L_\parallel^2} + \frac{z^2}{L_\perp^2}\right)^{-(4-D)\pi^2/18p^2}. \qquad (131)$$

Here we have used that in the I phase a difference in the soliton displacement is related to a shift of the phase $\phi(\mathbf{x})$ of the order parameter by $\phi(\mathbf{x}) - \phi(\mathbf{0}) = (2\pi/p)(z - u(\mathbf{x}) + u(\mathbf{0}))/\ell$.

In the opposite case where $\xi_\parallel \gg \ell$, the lattice potential V_L should be irrelevant since it averages to zero on scales larger than ℓ for geometric reasons. This corresponds to the situation above the roughening transition, $\Delta_0 > \Delta_{0,c}$, and now the original periodic medium (instead of the soliton lattice) is described by the Hamiltonian (1) with $V_L = 0$ since the misfit can now be shifted away as mentioned above. Therefore, the correlation function has to show a crossover to a behavior which is given by equation (131) where the Larkin lengths of the soliton lattice become that of the original periodic medium, $L_\parallel, L_\perp \to L_\Delta$. The exponent of the algebraic decay in equation (131) goes over to $-(4 - D)\pi^2/18$.

7 Experimental implications

Having established the possibility of a disorder driven roughening transition for various systems which can be

described in terms of elastic objects, we discuss now the experimental consequences of our results. To begin with, we comment on how the transition may be approached for a sample with *fixed* disorder strength. In general, for both elastic manifolds and periodic elastic media one may expect that the bare pinning strengths v_0 and Δ_0 depend also on temperature. Hence the transition should be reachable by changing the temperature T for appropriate T-dependencies of both pinning strengths. The precise T-dependence of the parameters is model dependent and, therefore, we will give only some general arguments and typical examples. Close to the condensation temperature T_c of the system where the intrinsic width of the elastic manifold becomes much larger than the periodicity of the lattice, $\xi_0 \gg a_0$, we expect a very weak influence of the crystal potential. An example are domain walls in magnets where T_c is the Curie temperature. For Peierls barriers which appear, *e.g.*, for domain walls in ferroelastics or solitons in incommensurate phases, one expects an exponentially decreasing influence of the lattice potential, $v_0 \sim e^{-C\xi_0}$.

The most prominent example for periodic elastic media are charge density waves. In this case the critical ratio of the pinning strengths depend also on temperature since $v_0/\Delta_0^2 \sim \rho_1^{2+p}$ for $D = 3$ where the charge density amplitude ρ_1 changes with T and vanishes at the Peierls temperature. Thus, for not too large disorder, we can expect to see the roughening transition by increasing T for both elastic manifolds and periodic media.

Indications about which phase is present should be given by the creep behavior since at small driving forces the dynamics are governed by the static behavior of the elastic objects. Indeed, under the influence of a small driving force density f_{ex}, the motion of the elastic object is dominated by jumps between neighboring metastable states in the rough phase and between adjacent minima of the lattice potential in the flat phase. As has been discussed earlier [28,41,56], in both cases the creep velocity u is exponentially small,

$$u(f_{ex}) \sim \exp\left[-\frac{E_c}{T}\left(\frac{f_c}{f_{ex}}\right)^\kappa\right], \qquad (132)$$

where f_c denotes the maximal pinning force density of the dominating pinning mechanism and E_c the corresponding energy barrier. The creep exponent κ depends on the phase which is present and on the type of disorder under consideration, *i.e.* on the disorder correlator $R_0(\phi)$.

For periodic elastic media, we obtain in the rough unlocked and flat phase, respectively,

$$\kappa_{rough} = \frac{D-2}{2}, \quad \kappa_{flat} = D - 1. \qquad (133)$$

The pinning force density and the energy barrier in the rough phase are given by $f_c \approx \gamma L_\Delta^{-2}$ and $E_c \approx \gamma L_\Delta^{D-2}$, whereas in the commensurate flat phase they are $f_c \approx \gamma\xi_\parallel^{-2}$ and $E_c \approx \gamma\xi_\parallel^{D-2}$.

For elastic manifolds, the exponent κ depends on the type of disorder *via* the roughness exponent ζ, *i.e.* random

bond or random field disorder,

$$\kappa_{rough} = \frac{D-2+2\zeta}{2-\zeta}, \quad \kappa_{flat} = D - 1. \qquad (134)$$

In the rough phase, we obtain $E_c \sim \gamma\xi_0^2 L_R^{D-2}$ and $f_c \sim \gamma\xi_0 L_R^{-2}$, and in the flat phase $E_c \sim \gamma v^{(2-D)/2}$ and $f_c \sim \gamma v$ for an interface with short range interactions. For dipolar systems one has to replace the dimension D according to equation (109), which gives $\kappa^{RF} = 1$, $\kappa^{RB} = 0.6666$ for a two-dimensional interface in the rough phase and $\kappa = 1$ for a flat interface independent of the type of disorder. Therefore, in the RB case the phase of the interface can be determined by measuring κ.

A very recent experiment on driven domain walls [57] shows that the exponent κ can be measured very accurately. This should make it possible to distinguish experimentally between both phases in the random bond case. For periodic media, an experimental realization is given by charge density waves. Recently measured I-V curves of the conductor o-TaS$_3$ at temperatures below 1 K can be fitted by equation (132) with $\kappa = 1.5 - 2$ [58]. The experimentally observed tendency to larger κ for purer crystals is in agreement with equation (133) for $D = 3$.

8 Discussion and conclusions

In this paper we have studied the static behavior of oriented elastic objects subjected to both a random potential and a periodic potential from an underlying crystal lattice. Scaling arguments and a functional RG calculation in $D = 4 - \epsilon$ dimensions led us to the conclusion that the competition between both pinning effects induces a *continuous* roughening transition between a flat phase with finite displacements and a rough state with diverging displacements. While based on the same physical mechanism, the description of the transition turned out to be different for periodic elastic media and single elastic manifolds.

For periodic elastic media such as charge density waves or flux line lattices in high-T_c superconductors, the transition exists only above some critical ratio $p_c = l/a_0$ of the lattice constants of the medium and the crystal potential. In $D = 3$ we obtain $p_c = 6/\pi$ from the ϵ-expansion. Below p_c, a weak random potential is irrelevant and the medium remains flat. On the flat side, this transition is described by three independent critical exponents which obey the scaling relations for random field systems with a discrete symmetry of the order parameter. Although the situation is similar to the thermal roughening transition in two dimensions, where also logarithmic roughness exists in the rough phase, in the disorder driven case the existence of one universal stable fixed point describing the rough phase leads to a different RG flow. In contrast, for the thermal case the temperature axis represents a line of fixed points. Notice that in the disorder dominated system studied here, the important logarithmic roughness sets in only beyond the Fukuyama-Lee length L_Δ, whereas thermal roughness in two dimensions appears on all length scales.

In the case of elastic manifolds, the interplay between random potential and lattice pinning leads also to a *continuous* transition for $2 < D < 4$. We have obtained the exponent $\nu_\parallel = 1/2\sqrt{\epsilon}$ for the divergence of the correlation length, which has to lowest order in ϵ the same form as that of the thermal roughening transition if $\epsilon = 2 - D$. For both random field and random bond systems, elastic manifolds show a superuniversal logarithmic roughness *at* the transition.

For $D = 2$ the interface is always asymptotically rough. At the upper critical dimension $D = 4$ an arbitrarily small lattice pinning produces a flat interface due to sub-logarithmic roughness in the absence of lattice effects. A diverging correlation length $\xi_\parallel$ appears on both sides of the transition. On the rough side $\xi_\parallel$ sets the length scale for the crossover from logarithmic to algebraic roughness.

Recently, the exact ground state of interfaces in the three-dimensional random bond, cubic lattice Ising model has been studied numerically [59]. For interfaces oriented along the {100} direction, a roughening transition at finite disorder strength from an almost flat to a rough phase has been observed whereas interfaces along the {111} direction remain always rough. Although our scaling arguments yield even for interfaces along the {100} direction no transition, one has to take into account the finite system sizes used in the numerical calculation. Indeed, we expect a flat behavior of the interface width up to the scale L_R, which is exponentially large for weak disorder in $D = 2$, hence probably leading to a flat 'phase' at sufficiently weak disorder in finite systems.

More recently, also the replica Hamiltonian for periodic media with $R_0(\phi) \sim \cos(\phi)$, $N = 1$, has been studied using the Gaussian variational method for $p = 1$, $2 \leq D < 4$ [60] and for $p = 1/2$, $D = 3$ [13]. Both analysis yield a self-consistency equation for the effective mass of the field $\phi(\mathbf{x})$ in terms of the disorder strength. Solutions of this equation exist only for v_0 above a particular value $v_{0,c}$, which is then identified with the phase boundary. At this phase boundary the effective mass remains *finite* corresponding to a first order transition. Moreover, the threshold $v_{0,c}$ is non-vanishing in spite of $p < p_c$. As we have shown by scaling arguments and the RG calculation, these results cannot be correct in the case of weak disorder. To understand the origin of these inconsistent results, we note that the derivation of the implicit equation is based on the assumption of a replica symmetric solution for the rough phase, hence corresponding to the perturbative result of Larkin. In the rough phase, for the correct logarithmic roughness on scales beyond the Larkin length L_Δ, replica symmetry breaking is needed within the variational approach. Since this logarithmic scaling on asymptotic scales is essential for the existence of a critical p_c, the replica symmetric determination of the effective mass cannot reproduce our RG result. In addition, the self-consistency equation cannot expected to be valid in the vicinity of a second order transition since it does not capture the physics on scales $\xi_\parallel \gg L_\Delta$ correctly. On the other hand, it should be noted that the variational approach, in contrast to the RG, does not depend on the assumption of weak pinning, hence de-
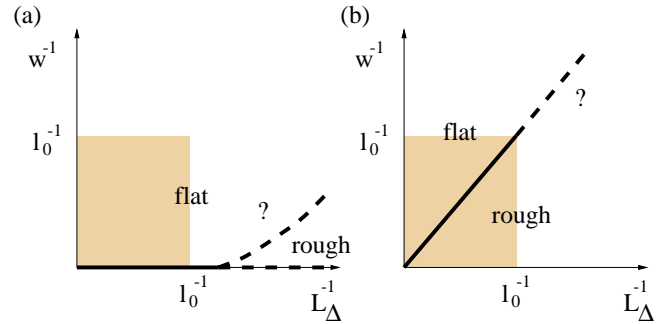
Fig. 9. Speculative phase diagrams including also the case of strong pinning where $w \sim v_0^{-1/2}$ and $L_\Delta \sim \Delta_0^{-1/(4-D)}$ become of the order of $l_0 =$max(a_0, ξ_0) for (a) $p < p_c$ and (b) $p > p_c$. In the shaded region the RG is expected to be valid. Dashed lines represent possible locations of the roughening transition which may be of first order outside the validity region of the RG.

scribing the system perhaps correctly in the case of strong pinning. However, the variational approach remains an uncontrolled approximation.

For $p < p_c$, the correlation length $\xi_\parallel$ has to diverge for $v_0 \to v_{0,c} = 0$. Now we address the question of the corresponding exponent $\nu_\parallel$. For this transition, there exists no unstable fixed point of the RG equations. As a first step towards an answer of this problem, one can calculate self-consistently an effective mass. To extend the validity range of the self-consistency equation derived in references [13,60] to weak disorder, we have taken into account the correct asymptotic roughness by using the RG result for the case where $v_0 = 0$. Then the solution for the effective mass depends on p. For $p < p_c$ the mass remains always finite for $v_0 > 0$ and vanishes *continuously* as $v_0 = 0$ is approached, leading to the exponent $\nu_\parallel = 1/2(1 - p^2/p_c^2)$ [61]. If $p > p_c$, the mass remains finite until $v_{0,c} > 0$, where a solution ceases to exist. In the latter case our RG treatment applies. We believe that the second order nature of the transition for $p < p_c$ is correctly given by our self-consistency condition, but the exponent $\nu_\parallel$ estimated from this condition should not be taken seriously.

The preceding discussion can be summarized in a speculative phase diagram, which includes also the strong pinning case, see Figure 9. If the pinning potentials are strong enough such that the characteristic scales $w \sim v_0^{-1/2}$ and $L_\Delta \sim \Delta_0^{-1/(4-D)}$ become of the order of max(a_0, ξ_0), a first order transition may appear.

In our study of periodic media we have not attempted to include the effect of topological defects. These can be considered if we treat $\phi(\mathbf{x})$ as a multi-valued field which may jump by $\pm 2\pi$ at surfaces which are bounded by vortex lines. Including these defects, qualitatively we expect the following picture. For $\delta = 0 = v_0$ it has been argued recently that for weak enough disorder strength $\Delta_0 < \Delta_D$, the system is stable with respect to the formation of vortices [62–64]. However, vortex lines will proliferate for $\Delta_0 > \Delta_D$. At present it is not clear whether

the corresponding transition is continuous or first order. For $\delta = 0$ but $v_0 > 0$ we expect that this transition extends to a line $\Delta_D(v_0)$ until v_0 reaches a critical value v_D with $\Delta_D(v_D) = \Delta_c(v_D)$ (see Fig. 7). For larger v_0 the transition is probably in the universality class of the p-state clock model in a random field, which has an upper critical dimension $d_c = 6$. For $p = 2$ (Ising like case) the transition is of second order [65]. A non-zero value of δ will in general increase the size of the incommensurate phase, as schematically sketched in Figure 8.

References

1. P.M. Chaikin, T.C. Lubensky, *Principles of condensed matter physics* (Cambridge University Press, Cambridge, 1995).
2. P.E. Wolf, F. Gallet, S. Balibar, E. Rolley, Ph. Nozières, J. Phys. France **46**, 1987 (1985).
3. J.D. Weeks, in *Ordering in Strongly Fluctuating Systems*, edited by T. Riste (Plenum, 1980).
4. H. van Beijeren, I. Nolden, in *Structure and Dynamics of Surfaces II*, edited by W. Schrommers, P. von Blanckenhagen (Springer, Berlin, 1987).
5. H. Fröhlich, Proc. R. Soc. London, Ser. A **223**, 296 (1954).
6. G. Grüner, *Density waves in solids* (Addison-Wesley, Reading, Massachusetts, 1994).
7. P. Bak, R. Bruinsma, Phys. Rev. Lett. **49**, 249 (1982).
8. V. Dvorak, in *Proc. Karpacz Winter School of Theoretical Physics*, edited by A. Pekalski, J. Przystawa (Berlin, Springer, 1979).
9. E.Y. Andrei *et al.*, Phys. Rev. Lett. **60**, 2765 (1988).
10. R. Seshadri, R.M. Westervelt, Phys. Rev. B **46**, 5142 (1992).
11. L. Balents, D.R. Nelson, Phys. Rev. B **52**, 12951 (1995).
12. S. Nieber, H. Kronmüller, Physica C **210**, 188 (1993).
13. S.V. Fridrikh, E.M. Terentjev, Phys. Rev. Lett. **79**, 4661 (1997).
14. D.J. Wallace, Field theories of surfaces, in *Gauge Theories and Experiments at High Energies*, edited by K.C. Bowler, D.G. Sutherland, (SUSSP Publications, Edinburgh, 1980).
15. I. Montvay, G. Münster, *Quantum Fields on a Lattice* (Cambridge University Press, Cambridge, 1994).
16. S.T. Chui, J.D. Weeks, Phys. Rev. B **14**, 4978 (1976).
17. H.J.F. Knops, Phys. Rev. Lett. **39**, 766 (1977).
18. J. Jose, Phys. Rev. D **14**, 2826 (1976).
19. A. Luther, I. Peshel, Phys. Rev. B **12**, 3908 (1975).
20. J.M. Kosterlitz, J. Phys. C **10**, 3753 (1977).
21. G. Forgacs, R. Lipowsky, T.M. Nieuwenhuizen, The behavior of interfaces in ordered and disordered systems, in *Phase Transitions and Critical Phenomena*, edited by C. Domb, J.L. Lebowitz (Academic Press, London, 1991), Vol. 14.
22. D.S. Fisher, M.E. Fisher, Phys. Rev. B **25**, 3192 (1982).
23. T. Halpin-Healy, Y.-C. Zhang, Phys. Rep. **254**, 215 (1995).
24. J. Villain, J. Phys. France **43**, L551 (1982).
25. G. Grinstein, S.K. Ma, Phys. Rev. Lett. **49**, 685 (1982).
26. K. Binder, Z. Phys. B **50**, 343 (1983).
27. J. Villain, Phys. Rev. Lett. **52**, 1543 (1984).
28. L.B. Ioffe, V.M. Vinokur, J. Phys. C **20**, 6149 (1987).
29. T. Nattermann, Europhys. Lett. **4**, 1241 (1987).
30. T. Nattermann, Y. Shapir, I. Vilfan, Phys. Rev. B **42**, 8577 (1990).
31. T. Nattermann, I. Vilfan, Phys. Rev. Lett. **61**, 223 (1988).
32. T. Nattermann *et al.*, J. Phys. II France **2**, 1483 (1992).
33. T. Nattermann, Z. Phys. B **54**, 247 (1984).
34. T. Nattermann, Phys. Stat. Sol. (b) **132**, 125 (1985).
35. J. P. Bouchaud, A. Georges, Phys. Rev. Lett. **68**, 3908 (1992).
36. T. Emig, T. Nattermann, Phys. Rev. Lett. **79**, 5090 (1997).
37. T. Emig, T. Nattermann, Phys. Rev. Lett. **81**, 1469 (1998).
38. T. Giamarchi, P. Le Doussal, Phys. Rev. Lett. **72**, 1530 (1994).
39. T. Giamarchi, P. Le Doussal, Phys. Rev. B **52**, 1242 (1995).
40. I. Morgenstern, K. Binder, R.M. Hornreich, Phys. Rev. B **23**, 287 (1981).
41. T. Nattermann, Phys. Rev. Lett. **64**, 2454 (1990).
42. U. Schulz, J. Villain, E. Brézin, H. Orland, J. Stat. Phys. **51**, 1 (1988).
43. L. Balents, D.S. Fisher, Phys. Rev. B **48**, 5949 (1993).
44. L. Balents, M. Kardar, Phys. Rev. B **49**, 13030 (1994).
45. D.S. Fisher, Phys. Rev. Lett. **56**, 1964 (1986).
46. T. Nattermann, H. Leschhorn, Europhys. Lett. **14**, 603 (1991).
47. J. Lajzerowicz, Ferroelectrics **24**, 179 (1980).
48. T. Nattermann, J. Phys. C **16**, 4125 (1983).
49. J. Villain, J. Phys. France **46**, 1843 (1985).
50. T. Nattermann, J. Villain, Phase Transit. **11**, 5 (1988).
51. A. Patashinsky, V. Pokrovsky, *Fluctuation Theory of Phase Transitions* (Pergamon Press, 1979).
52. V.L. Pokrovsky, A.L. Talapov, Phys. Rev. Lett. **42**, 65 (1979).
53. B. Horovitz, T. Bohr, J.M. Kosterlitz, H.J. Schulz, Phys. Rev. B **28**, 6596 (1983).
54. P. Nozières, Shape and growth of crystals, in *Solids far from Equilibrium*, edited by C. Godrèche (Cambridge University Press, Cambridge, 1992).
55. D.A. Huse, M.E. Fisher, Phys. Rev. B **29**, 239 (1984).
56. G. Blatter, M.V. Feigel'man, V.B. Geshkenbein, A.I. Larkin, V.M. Vinokur, Rev. Mod. Phys. **66**, 1125 (1994).
57. S. Lemerle *et al.*, Phys. Rev. Lett. **80**, 849 (1998).
58. S.V. Zaitsev-Zotov, G. Remenyi, P. Monceau, Phys. Rev. Lett. **78**, 1098 (1997).
59. M.J. Alava, P.M. Duxbury, Phys. Rev. B **54**, 14990 (1996).
60. T. Sasada, J. Phys. Soc. Jpn **65**, 2889 (1996).
61. T. Emig, T. Nattermann, unpublished .
62. M. Gingras, D. A. Huse, Phys. Rev. B **53**, 15193 (1996).
63. J. Kierfeld, T. Nattermann, T. Hwa, Phys. Rev. B **55**, 626 (1997).
64. D.S. Fisher, Phys. Rev. Lett. **78**, 1964 (1997).
65. T. Nattermann, P. Rujan, Int. J. Mod. Phys. B **3**, 1597 (1989).